

Proximal Methods for Sparse Optimal Scoring and Discriminant Analysis

Summer Atkins¹, Gudmundur Einarsson², Brendan Ames³, and Line Clemmensen²

¹Department of Mathematics, University of Florida, PO Box 118105, Gainesville, FL 32611-8105, srnatkins@ufl.edu

²Department of Applied Mathematics and Computer Science, Technical University of Denmark, Building 324, 2800 Kongens Lyngby, Denmark, {guei, lkhc}@dtu.dk

³Department of Mathematics, University of Alabama, Box 870350, Tuscaloosa, AL 35487-0350, bpames@ua.edu

September 20, 2019

Abstract

Linear discriminant analysis (LDA) is a classical method for dimensionality reduction, where discriminant vectors are sought to project data to a lower dimensional space for optimal separability of classes. Several recent papers have outlined strategies, based on exploiting sparsity of the discriminant vectors, for performing LDA in the high-dimensional setting where the number of features exceeds the number of observations in the data. However, many of these proposed methods lack scalable methods for solution of the underlying optimization problems. We consider an optimization scheme for solving the sparse optimal scoring formulation of LDA based on block coordinate descent. Each iteration of this algorithm requires update of a scoring vector, which admits an analytic formula, and update of the corresponding discriminant vector, which requires solution of a convex subproblem; we will propose several variants of this algorithm where the proximal gradient method or the alternating direction method of multipliers is used to solve this subproblem. We show that the per-iteration cost of these methods scales linearly in the dimension of the data provided restricted regularization terms are employed, and cubically in the dimension of the data in the worst case. Furthermore, we establish that when this block coordinate descent framework generates convergent subsequences of iterates, then these subsequences converge to the stationary points of the sparse optimal scoring problem. We demonstrate the effectiveness of our new methods with empirical results for classification of Gaussian data and data sets drawn from benchmarking repositories, including time-series and multispectral X-ray data, and provide **Matlab** and **R** implementations of our optimization schemes.

1 Introduction

Sparse discriminant techniques have become popular in the last decade due to their ability to provide increased interpretation as well as predictive performance for high-dimensional problems where few observations are present. These approaches typically build upon successes from sparse linear regression, in particular the LASSO and its variants (see [19, Section 3.4.2] and [20]), by augmenting existing schemes for linear discriminant analysis (LDA) with sparsity-inducing regularization terms, such as the ℓ_1 -norm and elastic net.

Thus far, little focus has been put on the optimization strategies of these sparse discriminant methods, nor their computational cost. We propose three novel optimization strategies to obtain discriminant directions in the high-dimensional setting where the number of observations n is much smaller than the ambient dimension p or when features are highly correlated, and analyze the convergence properties of these methods. The methods are proposed for multi-class sparse discriminant analysis using the sparse optimal scoring formulation with elastic net penalty proposed in [10]; adding both the ℓ_1 - and ℓ_2 -norm penalties gives

sparse solutions which, in particular, are competitive when high correlations exist in feature space due to the grouping behaviour of the ℓ_2 -norm. The first two strategies are proximal gradient methods based on modification of the (fast) iterative shrinkage algorithm [4] for linear inverse problems. The third method uses a variant of the alternating direction method of multipliers similar to that proposed in [2]. We will see that these heuristics allow efficient classification of high-dimensional data, which was previously impractical using the current state of the art for sparse discriminant analysis. For example, if a diagonal or low-rank Tikhonov regularization term is used and the number of observations is very small relative to p , then the per-iteration cost of each of our algorithms is $\mathcal{O}(p)$; that is, the per-iteration cost of our approach scales linearly with the number of features of our data. Finally, we provide implementations of our algorithms in the form of the R package **accSDA**(see [12]) and Matlab software ¹.

1.1 Existing approaches for sparse LDA

We begin with a brief overview of existing sparse discriminant analysis techniques. Methods such as [14,34,36] assume independence between the features in the given data. This can lead to poor performance in terms of feature selection as well as predictions, in particular when high correlations exist. Thresholding methods such as [32], although proven to be asymptotically optimal, ignore the existing multi-linear correlations when thresholding low correlation estimates. Thresholding, furthermore, does not guarantee an invertible correlation matrix, and often pseudo-inverses must be utilized.

For two-class problems, the results of [23] established an equivalence between the three methods described in [10,22,37]. These three approaches are formulated as constrained versions of Fisher’s discriminant problem, the optimal scoring problem, and a least squares formulation of linear discriminant analysis, respectively. For scaled regularization parameters, [23] showed that they all behave asymptotically as Bayes rules. Another two-class sparse linear discriminant method is the linear programming discriminant method proposed in [7], which finds an ℓ_1 -norm penalized estimate of the product between covariance matrix and difference in means.

The sparse optimal scoring (SOS) problem was originally formulated in [10] as a multi-class problem seeking at most $K - 1$ sparse discriminating directions, whereas [23] was formulated for binary problems. Mai and Zou later proposed a multi-class sparse discriminant analysis (MSDA) based on the Bayes rule formulation of linear discriminant analysis in [24]. It imposes only the ℓ_1 -norm penalty, whereas the SOS imposes an elastic net penalty (ℓ_1 - plus ℓ_2 -norm). Adding the ℓ_2 -norm can give better predictive performance, in particular when very high correlations exist in data. MSDA, furthermore, finds all discriminative directions at once, whereas SOS finds them sequentially via deflation. A sequential solution can be an advantage if the number of classes is high, and a solution involving only a few directions (the most discriminating ones) is needed. On the other hand, if K is small, finding all directions at once, may be advantageous, in order to not propagate errors in a sequential manner.

Finally, the zero-variance sparse discriminant analysis approach of [2] reformulates the sparse discriminant analysis problem as an ℓ_1 -penalized nonconvex optimization problem in order to sequentially identify discriminative directions in the null-space of the pooled within-class scatter matrix. Most relevant for our discussion here is the use of proximal methods to approximately solve the nonconvex optimization problems in [2]; we will adopt a similar approach for solving the SOS problem.

2 Proximal Methods for Sparse Discriminant Analysis

In this section, we describe a block coordinate descent approach for (approximately) solving the sparse optimal scoring problem for linear discriminant analysis. Proposed in [18], the optimal scoring problem recasts linear discriminant analysis as a generalization of linear regression where both the response variable, corresponding to an optimal labeling or scoring of the classes, and linear model parameters, which yield the discriminant vector, are sought. Specifically, suppose that we have the $n \times p$ data matrix \mathbf{X} , where the rows of \mathbf{X} correspond to observations in \mathbf{R}^p sampled from one of K classes; we assume that the data has been centered so that the sample mean is the zero vector $\mathbf{0} \in \mathbf{R}^p$. Optimal scoring generates a sequence of discriminant vectors and conjugate scoring vectors as follows. Suppose that we have identified the first

¹Available at <http://bpames.people.ua.edu/software>

$k - 1$ discriminant vectors $\beta_1, \dots, \beta_{k-1} \in \mathbf{R}^p$ and scoring vectors $\theta_1, \dots, \theta_{k-1} \in \mathbf{R}^K$. To calculate the k th discriminant vector β_k and scoring vector θ_k , we solve the optimal scoring criterion problem

$$\begin{aligned} \arg \min_{\theta \in \mathbf{R}^K, \beta \in \mathbf{R}^p} \quad & \|Y\theta - X\beta\|^2 \\ \text{s.t.} \quad & \frac{1}{n}\theta^T Y^T Y \theta = 1, \quad \theta^T Y^T Y \theta_\ell = 0 \quad \forall \ell < k, \end{aligned} \quad (1)$$

where Y denotes the $n \times K$ indicator matrix for class membership, defined by $y_{ij} = 1$ if the i th observation belongs to the j th class, and $y_{ij} = 0$ otherwise, and $\|\cdot\| : \mathbf{R}^n \rightarrow \mathbf{R}$ denotes the vector ℓ_2 -norm on \mathbf{R}^n defined by $\|y\| = \sqrt{y_1^2 + y_2^2 + \dots + y_n^2}$ for all $y \in \mathbf{R}^n$. We direct the reader to [18] for further details regarding the derivation of (1). A variant of the optimal scoring problem which employs regularization via the elastic net penalty function is proposed in [10]. As before, suppose that we have identified the first $k - 1$ discriminant vectors $\beta_1, \dots, \beta_{k-1}$ and scoring vectors $\theta_1, \dots, \theta_{k-1}$. We calculate the k th sparse discriminant vector β_k and scoring vector θ_k as the optimal solutions of the optimal scoring criterion problem

$$\begin{aligned} \arg \min_{\theta \in \mathbf{R}^K, \beta \in \mathbf{R}^p} \quad & \|Y\theta - X\beta\|^2 + \gamma \beta^T \Omega \beta + \lambda \|\beta\|_1 \\ \text{s.t.} \quad & \frac{1}{n}\theta^T Y^T Y \theta = 1, \quad \theta^T Y^T Y \theta_\ell = 0 \quad \forall \ell < k, \end{aligned} \quad (2)$$

where $\|\cdot\|_1 : \mathbf{R}^p \rightarrow \mathbf{R}$ denotes the vector ℓ_1 -norm on \mathbf{R}^p defined by $\|x\|_1 = |x_1| + |x_2| + \dots + |x_p|$ for all $x \in \mathbf{R}^p$, $Y \in \mathbf{R}^{n \times K}$ is again the indicator matrix for class membership, λ and γ are nonnegative tuning parameters, and Ω is a $p \times p$ positive definite matrix. That is, (2) is the result of adding regularization to the optimal scoring problem using a linear combination of the Tikhonov penalty term $\beta^T \Omega \beta$ and the ℓ_1 -norm penalty $\|\beta\|_1$; we will provide further discussion regarding the choice of Ω in Section 2.4. The optimization problem (2) is nonconvex, due to the presence of nonconvex spherical constraints. As such, we do not expect to find a globally optimal solution of (2) using iterative methods. Clemmensen et al. propose a block coordinate descent method to iteratively approximate solutions of (2) is proposed in [10]. Specifically, suppose that we have an estimate (θ^t, β^t) of (θ_k, β_k) . To update θ^t , we fix $\beta = \beta^t$ and solve the optimization problem

$$\begin{aligned} \theta^{t+1} = \arg \min_{\theta \in \mathbf{R}^K} \quad & \|Y\theta - X\beta^t\|^2 \\ \text{s.t.} \quad & \frac{1}{n}\theta^T Y^T Y \theta = 1, \quad \theta^T Y^T Y \theta_\ell = 0 \quad \forall \ell < k. \end{aligned} \quad (3)$$

The subproblem (3) is nonconvex in θ , however, it is known that (3) admits an analytic solution and can be solved exactly in polynomial time. Indeed, we have the following lemma providing an analytic update formula for θ . Note that this update requires $\mathcal{O}(K^3 + pn)$ floating point operations to perform the necessary matrix products. See [10, Section 2.2] for more details.

Lemma 2.1 *The problem (3) has optimal solution*

$$\theta^{t+1} = s(I - Q_k Q_k^T D) D^{-1} Y^T X \beta^t, \quad (4)$$

where $D = \frac{1}{n} Y^T Y$, Q_k is the $K \times k$ matrix with columns consisting of the $k - 1$ scoring vectors $\theta_1, \dots, \theta_{k-1}$ and the all-ones vector $\mathbf{e} \in \mathbf{R}^K$, and s is a proportionality constant ensuring that $(\theta^{t+1})^T D \theta^{t+1} = 1$.

For completeness, we provide a proof of Lemma 2.1 in Appendix A. After we have updated θ^{t+1} , we obtain β^{t+1} by solving the unconstrained optimization problem

$$\beta^{t+1} = \arg \min_{\beta \in \mathbf{R}^p} \|Y\theta^{t+1} - X\beta\|^2 + \gamma \beta^T \Omega \beta + \lambda \|\beta\|_1. \quad (5)$$

That is, we update β^{t+1} by solving the generalized elastic net problem (5). It is suggested in [10] that (2) can be solved using the *least angle regression (LARS)* algorithm proposed in [38]. Unfortunately, this approach carries a computational cost on the order of $\mathcal{O}(mnp + m^3)$, where m is the desired number of nonzero coefficients, which is prohibitively expensive if both p and m are large. For example, if $m = cp$ for some constant $c \in (0, 1)$, then the per-iteration cost scales cubically with p . We should also note that coordinate descent methods have been widely adopted for calculation of elastic net regularized generalized

Algorithm 1: Block Coordinate Descent for SDA (2)

Data: Given initial scoring vectors $\theta_1^0, \theta_2^0, \dots, \theta_{K-1}^0 \in \mathbf{R}^K$

Result: Discriminant vectors $(\theta_1^*, \beta_1^*), (\theta_2^*, \beta_2^*), \dots, (\theta_{K-1}^*, \beta_{K-1}^*)$ calculated as approximate solutions of (2).

for $k = 1, 2, \dots, K - 1$

 Calculate the k th scoring and discriminant vector pair (θ_k^*, β_k^*) as the limit point of the sequence $\{(\theta_k^t, \beta_k^t)\}_{t=0}^\infty$ calculated as follows:

for $t = 0, 1, 2 \dots$ until converged

 Update β_k^t as the solution of (5) with $\theta = \theta_k^t$ using the solution returned by one of (3), (4), (6), and (5);

 Update θ_k^{t+1} by

$$w = (I - Q_k Q_k^T D) D^{-1} Y^T X \beta_k^t,$$
$$\theta_k^{t+1} = \frac{w}{\sqrt{w^T D w}};$$

end

end

linear models; see [16] for further details. However, we are unaware of any application of coordinate descent methods for solution of the elastic net regularized optimal scoring problem (2).

Our primary contribution is a collection of algorithms for solving the elastic net problem (5). Specifically, we specialize three classical algorithms, each based on the evaluation of proximal operators, to obtain novel numerical methods for solution of the sparse optimal scoring problem. We will see that these algorithms require significantly fewer computational resources than least angle regression if we exploit structure in the regularization parameter Ω .

2.1 Proximal Algorithms for the Generalized Elastic Net Problem

Given a convex function $f : \mathbf{R}^p \rightarrow \mathbf{R}$, the *proximal operator* $\text{prox}_f : \mathbf{R}^p \rightarrow \mathbf{R}^p$ of f is defined by

$$\text{prox}_f(\mathbf{y}) = \arg \min_{\mathbf{x} \in \mathbf{R}^p} \left\{ f(\mathbf{x}) + \frac{1}{2} \|\mathbf{x} - \mathbf{y}\|^2 \right\},$$

which yields a point that balances the competing objectives of being near \mathbf{y} while simultaneously minimizing f . The use of proximal operators is a classical technique in optimization, particularly as surrogates for gradient descent steps for minimization of nonsmooth functions. For example, consider the optimization problem

$$\min_{\mathbf{x} \in \mathbf{R}^p} f(\mathbf{x}) + g(\mathbf{x}), \tag{6}$$

where $f : \mathbf{R}^p \rightarrow \mathbf{R}$ is differentiable and $g : \mathbf{R}^p \rightarrow \mathbf{R}$ is potentially nonsmooth. That is, (6) minimizes an objective that can be decomposed as the sum of a differentiable function f and nonsmooth function g . To solve (6), the *proximal gradient method* performs iterations consisting of a step in the direction of the negative gradient $-\nabla f$ of the smooth part f followed by evaluation of the proximal operator of g : given iterate \mathbf{x}^t , we obtain the updated iterate \mathbf{x}^{t+1} by

$$\mathbf{x}^{t+1} = \text{prox}_{\alpha_t g}(\mathbf{x}^t - \alpha_t \nabla f(\mathbf{x}^t)), \tag{7}$$

where α_t is a step length parameter. If both f and g are differentiable and the step size α_t is small, then this approach reduces to the classical gradient descent iteration: $\mathbf{x}^{t+1} \approx \mathbf{x}^t - \alpha_t \nabla f(\mathbf{x}^t) - \alpha_t \nabla g(\mathbf{x}^t)$. We direct the reader to the recent survey article [31] for more details regarding the proximal gradient method and proximal operators in general.

Algorithm 2: Backtracking algorithm for ISTA

Data: Start with $L_0 > 0$ and scaling parameter $\eta > 1$.

Result: Minimizer \mathbf{x}^* of F .

for $t = 0, 1, 2 \dots$ until converged

for $k = 0, 1, 2 \dots$ until step size accepted

 Update step length

$$\bar{L} = \eta^k L_{t-1}, \quad \alpha = \frac{1}{\bar{L}};$$

 Update iterate using proximal gradient step (7):

$$\mathbf{x}^{t+1} = \text{prox}_{\bar{\alpha}g}(\mathbf{x}^t + \bar{\alpha}\nabla f(\mathbf{x}^t)).$$

 Determine whether to accept update or increment step length:

if $F(\mathbf{x}^{t+1}) \leq f(\mathbf{x}^t) + \nabla f(\mathbf{x}^t)^T(\mathbf{x}^{t+1} - \mathbf{x}^t) + \frac{\bar{L}}{2}\|\mathbf{x}^{t+1} - \mathbf{x}^t\|^2 + g(\mathbf{x}^{t+1})$

 Accept update: $L_t = \bar{L}$, $\alpha_t = \bar{\alpha}$. ;

break;

end

end

end

In [4], the authors consider a specialization of the proximal gradient method, called the *iterative soft-thresholding algorithm (ISTA)* to the ℓ_1 -regularized linear inverse problem

$$\min_{\mathbf{x} \in \mathbf{R}^n} \|\mathbf{A}\mathbf{x} - \mathbf{b}\|^2 + \lambda\|\mathbf{x}\|_1, \quad (8)$$

where $\mathbf{A} \in \mathbf{R}^{m \times n}$, $\mathbf{b} \in \mathbf{R}^m$ are known, and $\lambda > 0$ is a regularization parameter chosen by the user; \mathbf{b} is often a vector of noisy measurements of an unknown vector or signal \mathbf{x} by the sampling matrix \mathbf{A} . The primary contribution of [4] is an accelerated variant of ISTA, called *fast iterative soft-threshold (FISTA)*, and a convergence analysis establishing the non-asymptotic global rate of convergence of both ISTA and FISTA; we'll delay further discussion of FISTA until Section 2.2. Although motivated by the linear inverse problem (8), the analysis of [4] focuses on the more general problem of minimizing the sum $f + g$, where f is differentiable with Lipschitz continuous gradient and g is potentially nonsmooth. In this case, a Lipschitz constant of ∇f is used as a constant step size in (7) or the step length is chosen using a backtracking line search as in Algorithm 2. The following theorem establishes that the sequence of iterates generated converges sublinearly to the optimal function value of $F := f + g$ at a rate no worse than $\mathcal{O}(1/t)$; see [4, Theorem 3.1].

Theorem 2.1 *Let the function $F : \mathbf{R}^n \rightarrow \mathbf{R}$ be decomposable as $F(\mathbf{x}) = f(\mathbf{x}) + g(\mathbf{x})$, where f is differentiable with Lipschitz continuous gradient; let L be a Lipschitz constant such that $\|\nabla f(\mathbf{x}) - \nabla f(\mathbf{y})\| \leq L\|\mathbf{x} - \mathbf{y}\|$ for all $\mathbf{x}, \mathbf{y} \in \mathbf{R}^n$. Suppose that F has minimizer $\mathbf{x}^* \in \mathbf{R}^n$. Let $\{\mathbf{x}^t\}_{t=0}^\infty$ be the sequence of iterates generated by (7) with constant step size $\alpha = 1/L$ or by Algorithm 2. Then there exists a constant $c > 0$ such that*

$$F(\mathbf{x}^t) - F(\mathbf{x}^*) \leq \frac{cL\|\mathbf{x}^0 - \mathbf{x}^*\|^2}{t} \quad (9)$$

for all t .

Expanding the residual norm term $\|\mathbf{Y}\boldsymbol{\theta} - \mathbf{X}\boldsymbol{\beta}\|^2$ in the objective of (5) and dropping the constant term shows that (5) is equivalent to minimizing

$$F(\boldsymbol{\beta}) = \frac{1}{2}\boldsymbol{\beta}^T \mathbf{A}\boldsymbol{\beta} + \mathbf{d}^T \boldsymbol{\beta} + \lambda\|\boldsymbol{\beta}\|_1, \quad (10)$$

where $\mathbf{A} = 2(\mathbf{X}^T \mathbf{X} + \gamma\boldsymbol{\Omega})$ and $\mathbf{d} = -2\mathbf{X}^T \mathbf{Y}\boldsymbol{\theta}^{t+1}$. We can decompose F as $F(\boldsymbol{\beta}) = f(\boldsymbol{\beta}) + g(\boldsymbol{\beta})$, where $f(\boldsymbol{\beta}) = \frac{1}{2}\boldsymbol{\beta}^T \mathbf{A}\boldsymbol{\beta} + \mathbf{d}^T \boldsymbol{\beta}$ and $g(\boldsymbol{\beta}) = \lambda\|\boldsymbol{\beta}\|_1$. Note that F is strongly convex if the penalty matrix $\boldsymbol{\Omega}$ is positive

Algorithm 3: Proximal gradient method for solving the elastic net subproblem (10)

Data: Initial iterate β^0 and sequence of step lengths $\{\alpha_t\}_{t=0}^\infty$.

Result: Solution β^* of (5).

for $t = 0, 1, 2 \dots$ until converged

 Update gradient term by (12):

$$\mathbf{p}^t = \beta^t - \alpha_t(\mathbf{A}\beta^t + \mathbf{d});$$

 Update iterate using proximal gradient step (11):

$$\beta^{t+1} = \text{sign}(\mathbf{p}^t) \max\{|\mathbf{p}^t| - \lambda\alpha_t\mathbf{e}, \mathbf{0}\};$$

end

definite; in this case (10) has a unique minimizer. Note further that f is differentiable with $\nabla f(\beta) = \mathbf{A}\beta + \mathbf{d}$. Moreover, the proximal operator of the ℓ_1 -norm term $g(\beta) = \lambda\|\beta\|_1$ is given by

$$\text{prox}_{\lambda\|\cdot\|_1}(\mathbf{y}) = \text{sign}(\mathbf{y}) \max\{|\mathbf{y}| - \lambda\mathbf{e}, \mathbf{0}\} =: S_\lambda(\mathbf{y});$$

see [31, Section 6.5.2]. The proximal operator $S_\lambda = \text{prox}_{\lambda\|\cdot\|_1}$ is often called the *soft thresholding operator* (with respect to the threshold λ) and $\text{sign} : \mathbf{R}^p \rightarrow \mathbf{R}^p$ and $\max : \mathbf{R}^p \times \mathbf{R}^p \rightarrow \mathbf{R}^p$ are the element-wise sign and maximum mappings defined by

$$[\text{sign}(\mathbf{y})]_i = \text{sign}(y_i) = \begin{cases} +1, & \text{if } y_i > 0 \\ 0, & \text{if } y_i = 0 \\ -1, & \text{if } y_i < 0 \end{cases}$$

and $[\max(\mathbf{x}, \mathbf{y})]_i = \max(x_i, y_i)$. Using this decomposition, we can apply the proximal gradient method to generate a sequence of iterates $\{\beta^t\}$ by

$$\beta^{t+1} = \text{sign}(\mathbf{p}^t) \max\{|\mathbf{p}^t| - \lambda\alpha_t\mathbf{e}, \mathbf{0}\}, \quad (11)$$

where

$$\mathbf{p}^t = \beta^t - \alpha_t \nabla f(\beta^t) = \beta^t - \alpha_t(\mathbf{A}\beta^t + \mathbf{d}); \quad (12)$$

here, \mathbf{e} and $\mathbf{0}$ denote the all-ones and all-zeros vectors in \mathbf{R}^p , respectively. This proximal gradient algorithm with constant step lengths is summarized in Algorithm 3; Algorithm 2 can be modified to obtain a variant of Algorithm 3 that employs a backtracking line search. It is important to note that this update scheme is virtually identical to that of ISTA. Specifically, our problem and update formula differs only from that typically associated with ISTA in the presence of the Tikhonov regression term $\beta^T \Omega \beta$ in our model. As an immediate consequence, we see that the sequence of function values $\{F(\beta^t)\}$ generated by Algorithm 3, with an appropriate choice of step lengths $\{\alpha_t\}$, converges sublinearly to the optimal function value of (10) at a rate no worse than $\mathcal{O}(1/t)$ (compare to Theorem 2.1).

Theorem 2.2 *Let $\{\beta^t\}$ be generated by Algorithm 3 with initial iterate β^0 and constant step size $\alpha_t = \alpha \in (0, 1/\|\mathbf{A}\|)$ or step sizes chosen using the backtracking scheme given by Algorithm 2, where $\|\mathbf{A}\| = \lambda_{\max}(\mathbf{A})$ denotes the spectral norm of \mathbf{A} equal to the largest magnitude eigenvalue of \mathbf{A} . Suppose that β^* is a minimizer of F . Then there exists a constant c such that*

$$F(\beta^t) - F(\beta^*) \leq \frac{c\|\mathbf{A}\|\|\beta^0 - \beta^*\|^2}{t} \quad (13)$$

for any $t \geq 1$.

It is known that ISTA converges *linearly* when the objective function F is strongly convex (see [3, Chapter 10]). We will see that the strong convexity of the objective of (2) depends on the structure of the

regularization term $\mathbf{\Omega}$. When $\mathbf{\Omega}$ is full rank, then F is strongly convex. Therefore, the sequence of iterates generated by Algorithm 3 converges to the unique minimizer of (5) if the penalty parameter $\mathbf{\Omega}$ is chosen to be positive definite. If we choose $\mathbf{\Omega}$ to be positive semidefinite but not full rank, then F may not be strongly convex. In this case, Theorem 2.2 establishes that the sequence of iterates generated by Algorithm 3 converges sublinearly to the minimum value of (5) and any limit point of this sequence is a minimizer of (5). We will see that using such a matrix may have attractive computational advantages despite this loss of uniqueness.

It is reasonably easy to see that the quadratic term of F in (10) is differentiable and has Lipschitz continuous gradient with constant $L = \|\mathbf{A}\|$; this is the significance of the $\|\mathbf{A}\|$ term in (13). In order to ensure convergence in our proximal gradient method, we need to estimate $\|\mathbf{A}\|$ to choose a sufficiently small step size α . Computing this Lipschitz constant may be prohibitively expensive for large p ; one can typically calculate $\|\mathbf{A}\|$ to arbitrary precision using variants of the Power Method (see [17, Sections 7.3.1, 8.2]) at a cost of $\mathcal{O}(p^2 \log p)$ floating point operations. Instead, we could use an upper bound $\tilde{L} \geq L$ to compute our constant step size $\alpha = 1/\tilde{L} \leq 1/L$. For example, when $\mathbf{\Omega}$ is a diagonal matrix, we estimate $\|\mathbf{A}\|$ by

$$\|\mathbf{A}\| = 2\|\gamma\mathbf{\Omega} + \mathbf{X}^T \mathbf{X}\| \leq 2\gamma\|\text{diag}(\mathbf{\Omega})\|_\infty + 2\|\mathbf{X}\|_F^2 \approx \frac{1}{\alpha},$$

where $\text{diag}(\mathbf{M}) \in \mathbf{R}^p$ is the vector of diagonal entries of the matrix $\mathbf{M} \in \mathbf{R}^{p \times p}$. Here, we used the triangle inequality and the identity $\|\mathbf{X}^T \mathbf{X}\| \leq \|\mathbf{X}\|_F^2$, where $\|\mathbf{X}\|_F$ denotes the Frobenius norm of \mathbf{X} defined by $\|\mathbf{X}\|_F^2 = \sum_{i=1}^n \sum_{j=1}^p x_{ij}^2$. The Frobenius norm and, hence, this estimate of $\|\mathbf{A}\|$ can be computed using only $\mathcal{O}(np)$ floating point operations.

2.2 The Accelerated Proximal Gradient Method

The similarity of our method to iterative soft thresholding and, more generally, our use of proximal gradient steps to mimic the gradient method for minimization of our nonsmooth objective, suggests that we may be able to use momentum terms to accelerate convergence of our iterates. In particular, we modify the fast iterative soft thresholding algorithm (FISTA) described in [4, Section 4] to solve our subproblem. This approach extends a variety of accelerated gradient descent methods, most notably those of Nesterov [26–28], to minimization of composite convex functions; for further details regarding the acceleration process and motivation for why such acceleration is possible, we direct the reader to the references [1, 6, 15, 21, 30, 33, 35].

We accelerate convergence of our iterates by taking a proximal gradient step from an extrapolation of the last two iterates. Applied to (6), the accelerated proximal gradient method features updates of the form

$$\mathbf{y}^{t+1} = \mathbf{x}^t + \omega_t(\mathbf{x}^t - \mathbf{x}^{t-1}) \quad (14)$$

$$\mathbf{x}^{t+1} = \underset{\alpha g}{\text{prox}}(\mathbf{y}^{t+1} - \alpha \nabla f(\mathbf{y}^{t+1})), \quad (15)$$

where $\omega_t \in [0, 1)$ is an extrapolation parameter; a standard choice of this parameter is $t/(t+3)$. Applying this modification to our original proximal gradient algorithm yields Algorithm 4. Modifying the backtracking line search of Algorithm 2 to use the accelerated proximal gradient update yields Algorithm 5. It can be shown that the sequence of iterates generated by either of these algorithms converges in value to the optimal solution of (5) at rate $\mathcal{O}(1/t^2)$ (see [4, Theorem 4.4]).

Theorem 2.3 *Let $\{\beta^t\}$ be generated by Algorithm 4 and constant step size $\alpha_t = \alpha \in (0, 1/\|\mathbf{A}\|)$ or generated using backtracking line search by Algorithm 5 with initial iterate β^0 . Then there exists constant $c > 0$ such that*

$$F(\beta^t) - F(\beta^*) \leq \frac{c\|\mathbf{A}\|\|\beta^0 - \beta^*\|^2}{t^2} \quad (16)$$

for any $t \geq 1$ and minimizer β^* of F .

2.3 The Alternating Direction Method of Multipliers

We conclude by proposing a third algorithm for minimization of (10) based on the *alternating direction method of multipliers* (ADMM) for minimizing separable functions under linear coupling constraints. The

Algorithm 4: Accelerated proximal gradient method for solving (10) with constant step size

Data: Initial iterates $\beta^0 = \beta^1$, step length α , and sequence of extrapolation parameters $\{\omega_t\}_{t=0}^\infty$.

Result: Solution β^* of (5).

for $t = 1, 2 \dots$ until converged

 Update momentum term by (14):

$$\mathbf{y}^{t+1} = \beta^t + \omega_t(\beta^t - \beta^{t-1});$$

 Update gradient term by (12):

$$\mathbf{p}^{t+1} = \mathbf{y}^{t+1} - \alpha(\mathbf{A}\mathbf{y}^{t+1} + \mathbf{d});$$

 Update iterate using proximal gradient step (11):

$$\beta^{t+1} = \text{sign}(\mathbf{p}^{t+1}) \max\{|\mathbf{p}^{t+1}| - \lambda\alpha\mathbf{e}, \mathbf{0}\};$$

end

Algorithm 5: Accelerated proximal gradient method for solving (10) with backtracking line search

Data: Initial iterates $\beta^0 = \beta^{-1}$, initial Lipschitz constant $L_0 > 0$, scaling parameter $\eta > 1$, and sequence of extrapolation parameters $\{\omega_t\}_{t=0}^\infty$.

Result: Solution β^* of (5).

for $t = 0, 1, 2 \dots$ until converged

for $k = 0, 1, 2 \dots$ until step size accepted

 Update step length

$$\bar{L} = \eta^k L_{t-1}, \quad \alpha = \frac{1}{\bar{L}};$$

 Update iterate using accelerated proximal gradient step (11):

$$\mathbf{y}^{t+1} = \beta^t + \omega_t(\beta^t - \beta^{t-1})$$

$$\mathbf{p}^{t+1} = \mathbf{y}^{t+1} - \alpha(\mathbf{A}\mathbf{y}^{t+1} + \mathbf{d})$$

$$\beta^{t+1} = \text{sign}(\mathbf{p}^{t+1}) \max\{|\mathbf{p}^{t+1}| - \lambda\alpha\mathbf{e}, \mathbf{0}\};$$

 Determine whether to accept update or increment step length:

if $(\beta^{t+1} - \mathbf{y}^{t+1})^T \left(\frac{\bar{L}}{2} \mathbf{I} - \mathbf{A} \right) (\beta^{t+1} - \mathbf{y}^{t+1}) \geq 0$

 Accept update: set $L_t = \bar{L}$ and $\alpha_t = \bar{\alpha}$;

break;

end

end

end

ADMM solves problems of the form

$$\min_{\mathbf{x} \in \mathbf{R}^p, \mathbf{y} \in \mathbf{R}^m} \{f(\mathbf{x}) + g(\mathbf{y}) : \mathbf{A}\mathbf{x} + \mathbf{B}\mathbf{y} = \mathbf{c}\}, \quad (17)$$

via an approximate dual gradient ascent, where $f : \mathbf{R}^p \rightarrow \mathbf{R}$, $g : \mathbf{R}^m \rightarrow \mathbf{R}$, $\mathbf{A} \in \mathbf{R}^{r \times p}$, $\mathbf{B} \in \mathbf{R}^{r \times m}$, and $\mathbf{c} \in \mathbf{R}^r$; we direct the reader to the recent survey [5] for more details regarding the ADMM.

Recall that the minimization of the composite function F defined in (10) can be written as the unconstrained optimization problem

$$\min_{\beta \in \mathbf{R}^p} F(\beta) = \min_{\beta \in \mathbf{R}^p} \frac{1}{2} \beta^T \mathbf{A} \beta + \mathbf{d}^T \beta + \lambda \|\beta\|_1. \quad (18)$$

We can rewrite (18) in an equivalent form appropriate for the ADMM by splitting the decision variable $\beta \in \mathbf{R}^p$ as two new variables $\mathbf{x}, \mathbf{y} \in \mathbf{R}^p$ with an accompanying linear coupling constraint $\mathbf{x} = \mathbf{y}$. Under this change of variables, we can express (18) as

$$\begin{aligned} \min_{\mathbf{x}, \mathbf{y} \in \mathbf{R}^p} \quad & \frac{1}{2} \mathbf{x}^T \mathbf{A} \mathbf{x} - \mathbf{x}^T \mathbf{d} + \lambda \|\mathbf{y}\|_1 \\ \text{s.t.} \quad & \mathbf{x} - \mathbf{y} = \mathbf{0}; \end{aligned} \quad (19)$$

here, we have changed the sign of \mathbf{d} , i.e., we use $\mathbf{d} = +2\mathbf{X}^T \mathbf{Y} \boldsymbol{\theta}^{t+1}$, which will simplify later calculations. The ADMM generates a sequence of iterates using approximate dual gradient ascent steps as follows. The augmented Lagrangian of (19) is defined by

$$L_\mu(\mathbf{x}, \mathbf{y}, \mathbf{z}) = \frac{1}{2} \mathbf{x}^T \mathbf{A} \mathbf{x} - \mathbf{x}^T \mathbf{d} + \lambda \|\mathbf{y}\|_1 + \mathbf{z}^T (\mathbf{x} - \mathbf{y}) + \frac{\mu}{2} \|\mathbf{x} - \mathbf{y}\|^2$$

for all $\mathbf{x}, \mathbf{y}, \mathbf{z} \in \mathbf{R}^p$; here, $\mu > 0$ is a penalty parameter controlling the emphasis on enforcing feasibility of the primal iterates \mathbf{x} and \mathbf{y} . To approximate the gradient of the dual functional of (19), we alternately minimize the augmented Lagrangian with respect to \mathbf{x} and \mathbf{y} . We then update the dual variable \mathbf{z} by a dual ascent step using this approximate gradient.

Suppose that we have the iterates $(\mathbf{x}^t, \mathbf{y}^t, \mathbf{z}^t)$ after t steps of our algorithm. To update \mathbf{x} , we take

$$\mathbf{x}^{t+1} = \arg \min_{\mathbf{x} \in \mathbf{R}^p} L_\mu(\mathbf{x}, \mathbf{y}^t, \mathbf{z}^t) = \arg \min_{\mathbf{x} \in \mathbf{R}^p} \frac{1}{2} \mathbf{x}^T (\mu \mathbf{I} + \mathbf{A}) \mathbf{x} - \mathbf{x}^T (\mathbf{d} + \mu \mathbf{y}^t - \mathbf{z}^t).$$

Applying the first order necessary and sufficient conditions for optimality, we see that \mathbf{x}^{t+1} must satisfy

$$(\mu \mathbf{I} + \mathbf{A}) \mathbf{x}^{t+1} = \mathbf{d} + \mu \mathbf{y}^t - \mathbf{z}^t. \quad (20)$$

Thus, \mathbf{x}^{t+1} is obtained as the solution of a linear system. Note that the coefficient matrix $\mu \mathbf{I} + \mathbf{A}$ is independent of t ; we take the Cholesky decomposition of $\mu \mathbf{I} + \mathbf{A} = \mathbf{B} \mathbf{B}^T$ during a preprocessing step and obtain \mathbf{x}^{t+1} by solving the two triangular systems given by

$$\mathbf{B} \mathbf{B}^T \mathbf{x}^{t+1} = \mathbf{d} + \mu \mathbf{y}^t - \mathbf{z}^t.$$

When the generalized elastic net matrix $\boldsymbol{\Omega}$ is diagonal, or $\mathbf{M} := \mu \mathbf{I} + 2\gamma \boldsymbol{\Omega}$ is otherwise easy to invert, we can invoke the Sherman-Morrison-Woodbury formula (see [17, Section 2.1.4]) to solve this linear system more efficiently; more details will be provided in Section 2.4. In particular, we see that

$$(\mu \mathbf{I} + 2\gamma \boldsymbol{\Omega} + 2\mathbf{X}^T \mathbf{X})^{-1} = \mathbf{M}^{-1} - 2\mathbf{M}^{-1} \mathbf{X}^T (\mathbf{I} + 2\mathbf{X} \mathbf{M}^{-1} \mathbf{X}^T)^{-1} \mathbf{X} \mathbf{M}^{-1};$$

computing this inverse only requires computing the inverse of \mathbf{M} and the inverse of the $n \times n$ matrix $\mathbf{I} + 2\mathbf{X} \mathbf{M}^{-1} \mathbf{X}^T$.

Next \mathbf{y} is updated by

$$\mathbf{y}^{t+1} = \arg \min_{\mathbf{y} \in \mathbf{R}^p} L_\mu(\mathbf{x}^{t+1}, \mathbf{y}, \mathbf{z}^t) = \arg \min_{\mathbf{y}} \lambda \|\mathbf{y}\|_1 + \frac{\mu}{2} \|\mathbf{y} - \mathbf{x}^{t+1} - \mathbf{z}^t / \mu\|^2.$$

That is, \mathbf{y}^{t+1} is updated as the value of the soft thresholding operator of the ℓ_1 -norm at $\mathbf{z}^t / \mu + \mathbf{x}^{t+1}$:

$$\mathbf{y}^{t+1} = S_{\lambda/\mu}(\mathbf{x}^{t+1} + \mathbf{z}^t / \mu). \quad (21)$$

Finally, the dual variable \mathbf{z} is updated using the approximate dual ascent step

$$\mathbf{z}^{t+1} = \mathbf{z}^t + \mu(\mathbf{x}^{t+1} - \mathbf{y}^{t+1}). \quad (22)$$

This approach is summarized in Algorithm 6. It is well-known that the ADMM generates a sequence of iterates which converge linearly to an optimal solution of (17) under certain strong convexity assumptions on f and g and rank assumptions on \mathbf{A} and \mathbf{B} , all of which are satisfied by our problem (19) when $\boldsymbol{\Omega}$ is positive definite (see, for example, [11]). It follows that the sequence of iterates $\{\mathbf{x}^t, \mathbf{y}^t, \mathbf{z}^t\}$ generated by Algorithm 6 converges to a minimizer of $F(\beta)$; that is, $\mathbf{x}^t - \mathbf{y}^t \rightarrow \mathbf{0}$ and $F(\mathbf{x}^t), F(\mathbf{y}^t)$ converge linearly to the minimum value of F . If F is not strongly convex, then we should expect Algorithm (6) to generate a sequence of iterates that converge sublinearly in value to the optimal value of (5).

Algorithm 6: Alternating direction method of multipliers for solving (19)

Data: Start with initial iterates $\mathbf{x}^0 = \mathbf{y}^0$ and step length μ .

Result: Solution $\beta^* = \mathbf{x}^* = \mathbf{y}^*$ of (5).

for $t = 0, 1, 2 \dots$ until converged

 Update \mathbf{x} by (20):

$$(\mu \mathbf{I} + \mathbf{A})\mathbf{x}^{t+1} = \mathbf{d} + \mu \mathbf{y}^t - \mathbf{z}^t;$$

 Update \mathbf{y} using soft thresholding (21):

$$\mathbf{y}^{t+1} = S_{\lambda/\mu}(\mathbf{x}^{t+1} + \mathbf{z}^t/\mu);$$

 Update \mathbf{z} using approximate dual ascent (22):

$$\mathbf{z}^{t+1} = \mathbf{z}^t + \mu(\mathbf{x}^{t+1} - \mathbf{y}^{t+1});$$

end

2.4 Computational Requirements

To motivate the use of our proposed proximal methods for the minimization of (5), we briefly sketch the per-iteration computational costs of each of our methods. We will see that for certain choices of regularization parameters, the number of floating point operations needed for each iteration scales linearly with the size of the data.

The most expensive step of both the proximal gradient method (Algorithm 3) and the accelerated proximal gradient method (Algorithm 4) is the evaluation of the gradient ∇f . Given a vector $\beta \in \mathbf{R}^p$, the gradient at β is given by

$$\nabla f(\beta) = \mathbf{A}\beta = 2 \left(\mathbf{X}^T \mathbf{X} + \gamma \mathbf{\Omega} \right) \beta = 2 \mathbf{X}^T \mathbf{X} \beta + 2 \gamma \mathbf{\Omega} \beta.$$

The product $\mathbf{X}^T \mathbf{X} \beta$ can be computed using $\mathcal{O}(np)$ floating point operations (flops) by computing $\mathbf{y} = \mathbf{X} \beta$ and then $\mathbf{X}^T \mathbf{y}$. On the other hand, the product $\mathbf{\Omega} \beta$ requires $\mathcal{O}(p^2)$ flops for unstructured $\mathbf{\Omega}$. However, if we use a *structured* regularization parameter $\mathbf{\Omega}$ we can significantly decrease this computational cost. Consider the following examples:

- Suppose that $\mathbf{\Omega}$ is a diagonal matrix: $\mathbf{\Omega} = \text{Diag}(\mathbf{u})$ for some vector $\mathbf{u} \in \mathbf{R}_+^p$. Then the product $\mathbf{\Omega} \beta$ can be computed using $\mathcal{O}(p)$ flops: $(\mathbf{\Omega} \beta)_i = u_i \beta_i$. Moreover, we can estimate the Lipschitz constant $\|\mathbf{A}\|$ for use in choosing the step size α by $\|\mathbf{A}\| \leq 2\gamma \|\mathbf{\Omega}\| + 2\|\mathbf{X}\|_F^2 = 2\gamma \|\mathbf{u}\|_\infty + 2\|\mathbf{X}\|_F^2$, which requires $\mathcal{O}(np)$ flops, primarily to compute the norm $\|\mathbf{X}\|_F^2$.
- If the use of diagonal $\mathbf{\Omega}$ is inappropriate, we could store $\mathbf{\Omega}$ in factored form $\mathbf{\Omega} = \mathbf{R} \mathbf{R}^T$ where $\mathbf{R} \in \mathbf{R}^{p \times r}$, and r is the rank of $\mathbf{\Omega}$. In this case, we have $\mathbf{\Omega} \beta = \mathbf{R}(\mathbf{R}^T \beta)$, which can be computed at a cost of $\mathcal{O}(rp)$ flops. Thus, if we use a low-rank parameter $\mathbf{\Omega}$, say $r \leq \mathcal{O}(n)$, we can compute the gradient using $\mathcal{O}(np)$ flops. Similarly, we can estimate the step size α using $\|\mathbf{A}\| \leq 2\|\mathbf{R}\|_F^2 + 2\|\mathbf{X}\|_F^2$ (computed at a cost of $\mathcal{O}(rp + np)$ flops).

In either case, using a diagonal $\mathbf{\Omega}$ or low-rank factored $\mathbf{\Omega}$, each iteration of the proximal gradient method or the accelerated proximal gradient method requires $\mathcal{O}(np)$ flops. Similar improvements can be made if $\mathbf{\Omega}$ is tridiagonal, banded, sparse, or otherwise nicely structured.

Similarly, the use of structured $\mathbf{\Omega}$ can lead to significant improvements in computational efficiency in our ADMM algorithm. The main computational bottleneck of this method is the solution of the linear system in the update of \mathbf{x} :

$$(\mu \mathbf{I} + \mathbf{A})\mathbf{x}^{t+1} = \mathbf{d} + \mu \mathbf{y}^t - \mathbf{z}^t.$$

Without taking advantage of the structure of \mathbf{A} , we can solve this system using a Cholesky factorization preprocessing step (at a cost of $\mathcal{O}(p^3)$ flops) and substitution to solve the resulting triangular systems (at a

		Diagonal $\mathbf{\Omega}$	Rank r $\mathbf{\Omega}$	Full rank $\mathbf{\Omega}$
Proximal Gradient	∇f	$\mathcal{O}(np)$	$\mathcal{O}(rp + np)$	$\mathcal{O}(p^2)$
	Bound on $\ \mathbf{A}\ $	$\mathcal{O}(np)$	$\mathcal{O}(rp + np)$	$\mathcal{O}(p^2 \log p)$
ADMM	$(\mu \mathbf{I} + \mathbf{A})\mathbf{x} = \mathbf{b}$	$\mathcal{O}(n^3 + n^2p)$	$\mathcal{O}(n^3 + n^2p + r^2p)$	$\mathcal{O}(p^3)$

Table 1: Upper bounds on floating point operation counts for most time consuming steps of each algorithm.

cost of $\mathcal{O}(p^2)$ flops per-iteration). However, we can often use the Sherman-Morrison-Woodbury Lemma to solve this system more efficiently using the structure of \mathbf{A} . Indeed, fix t and let $\mathbf{b} = \mathbf{d} + \mu \mathbf{y}^t - \mathbf{z}^t$. Then we update \mathbf{x} by $\mathbf{x} = (\mu \mathbf{I} + \mathbf{A})^{-1} \mathbf{b}$. If $\mathbf{M} = \mu \mathbf{I} + 2\gamma \mathbf{\Omega}$ then we have

$$\begin{aligned}
(\mu \mathbf{I} + \mathbf{A})^{-1} &= \left(\mu \mathbf{I} + 2\gamma \mathbf{\Omega} + 2\mathbf{X}^T \mathbf{X} \right)^{-1} = \left(\mathbf{M} + 2\mathbf{X}^T \mathbf{X} \right)^{-1} \\
&= \mathbf{M}^{-1} - 2\mathbf{M}^{-1} \mathbf{X}^T \left(\mathbf{I} + 2\mathbf{X} \mathbf{M}^{-1} \mathbf{X}^T \right)^{-1} \mathbf{X} \mathbf{M}^{-1}.
\end{aligned}$$

The matrix $\mathbf{I} + 2\mathbf{X} \mathbf{M}^{-1} \mathbf{X}^T$ is $n \times n$, so we may solve any linear system with this coefficient matrix using $\mathcal{O}(n^3)$ flops; a further $\mathcal{O}(n^2p)$ flops are needed to compute the coefficient matrix if given \mathbf{M}^{-1} . Thus, the main computational burden of this update step is the inversion of the matrix \mathbf{M} . As before, we want to choose $\mathbf{\Omega}$ so that we can exploit its structure. Consider the following cases.

- If $\mathbf{\Omega} = \text{Diag}(\mathbf{u})$ is diagonal, then \mathbf{M} is also diagonal with

$$[\mathbf{M}^{-1}]_{ii} = \frac{1}{\mu + 2\gamma u_i}.$$

Thus, we require $\mathcal{O}(p)$ flops to compute $\mathbf{M}^{-1} \mathbf{v}$ for any vector $\mathbf{v} \in \mathbf{R}^p$.

- On the other hand, if $\mathbf{\Omega} = \mathbf{R} \mathbf{R}^T$, where $\mathbf{R} \in \mathbf{R}^{p \times r}$, then we may use the Sherman-Morrison-Woodbury identity to compute \mathbf{M}^{-1} :

$$\mathbf{M}^{-1} = \frac{1}{\mu} \mathbf{I} - \frac{2\gamma}{\mu^2} \mathbf{R} \left(\mathbf{I} + \frac{2\gamma}{\mu} \mathbf{R}^T \mathbf{R} \right)^{-1} \mathbf{R}^T.$$

Therefore, we can solve any linear system with coefficient matrix \mathbf{M} at a cost of $\mathcal{O}(r^2p)$ flops (for the formation and solution of the system with coefficient matrix $\mathbf{I} + \frac{2\gamma}{\mu} \mathbf{R}^T \mathbf{R}$).

In either case, we never actually compute the matrices \mathbf{M}^{-1} and $(\mu \mathbf{I} + \mathbf{A})^{-1}$ explicitly. Instead, we update \mathbf{x} as the solution of a sequence of linear systems and matrix-vector multiplications, at a total cost of $\mathcal{O}(n^2p)$ flops (in the diagonal case) or $\mathcal{O}((r^2 + n^2)p)$ flops (in the factored case). Thus, if the number of observations n is much smaller than the number of features p , then the per-iteration computation scales roughly linearly with p . Table 1 summarizes these estimates of per-iteration computational costs for each proposed algorithm. Further, we should note that these bounds on per-iteration cost assume that the iterates $\boldsymbol{\beta}$ and \mathbf{x} are dense; the soft-thresholding step of the proximal gradient algorithm typically induces $\boldsymbol{\beta}$ containing many zeros, suggesting that further improvements can be made by using sparse arithmetic.

2.5 Convergence of our block coordinate descent method

In this section, we investigate the convergence properties of our block coordinate descent method (Algorithm 1). Our two main results, Theorem 2.4 and Theorem 2.5, are specializations of standard results for alternating minimization algorithms; we provide proofs of these results as appendices.

We first note that the Lagrangian $L : \mathbf{R}^K \times \mathbf{R}^p \times \mathbf{R} \times \mathbf{R}^{k-1} \rightarrow \mathbf{R}$ of (2) is given by

$$L(\boldsymbol{\theta}, \boldsymbol{\beta}, \psi, \mathbf{v}) = \|\mathbf{Y}\boldsymbol{\theta} - \mathbf{X}\boldsymbol{\beta}\|^2 + \gamma\boldsymbol{\beta}^T \boldsymbol{\Omega} \boldsymbol{\beta} + \lambda\|\boldsymbol{\beta}\|_1 \\ + \psi(\boldsymbol{\theta}^T \mathbf{Y}^T \mathbf{Y} \boldsymbol{\theta} - n) + \mathbf{v}^T \mathbf{U} \boldsymbol{\theta},$$

where $\mathbf{U}^T = (\mathbf{Y}^T \mathbf{Y} \boldsymbol{\theta}_1, \mathbf{Y}^T \mathbf{Y} \boldsymbol{\theta}_2, \dots, \mathbf{Y}^T \mathbf{Y} \boldsymbol{\theta}_{k-1})$. Note that the Lagrangian is *not* a convex function in general. However, L is the sum of the (possibly) nonconvex quadratic $\|\mathbf{Y}\boldsymbol{\theta} - \mathbf{X}\boldsymbol{\beta}\|^2 + \psi(\boldsymbol{\theta}^T \mathbf{Y}^T \mathbf{Y} \boldsymbol{\theta} - n) + \gamma\boldsymbol{\beta}^T \boldsymbol{\Omega} \boldsymbol{\beta} + \mathbf{v}^T \mathbf{U} \boldsymbol{\theta}$ and the convex nonsmooth function $\lambda\|\boldsymbol{\beta}\|_1$; therefore, L is subdifferentiable, with subdifferential at $(\boldsymbol{\beta}, \boldsymbol{\theta})$ given by the sum of the gradient of the smooth term at $(\boldsymbol{\beta}, \boldsymbol{\theta})$ and the subdifferential of the convex nonsmooth term at $(\boldsymbol{\beta}, \boldsymbol{\theta})$.

We now provide our first convergence result, specifically, that Algorithm 1 generates a convergent sequence of function values.

Theorem 2.4 *Suppose that the sequence of iterates $\{(\boldsymbol{\theta}^t, \boldsymbol{\beta}^t)\}_{t=0}^\infty$ is generated by Algorithm 1. Then the sequence of objective function values $\{F(\boldsymbol{\theta}^t, \boldsymbol{\beta}^t)\}_{t=0}^\infty$ defined by $F(\boldsymbol{\theta}, \boldsymbol{\beta}) := \|\mathbf{Y}\boldsymbol{\theta} - \mathbf{X}\boldsymbol{\beta}\|^2 + \gamma\boldsymbol{\beta}^T \boldsymbol{\Omega} \boldsymbol{\beta} + \lambda\|\boldsymbol{\beta}\|_1$ is convergent.*

We include a proof of Theorem 2.4 in Appendix B.

We also have the following theorem, which establishes that every convergent subsequence of $\{(\boldsymbol{\theta}^t, \boldsymbol{\beta}^t)\}_{t=1}^\infty$ converges to a stationary point of (2).

Theorem 2.5 *Let $\{(\boldsymbol{\theta}^t, \boldsymbol{\beta}^t)\}_{t=1}^\infty$ be the sequence of points generated by Algorithm 1. Suppose that $\{(\boldsymbol{\theta}^{t_j}, \boldsymbol{\beta}^{t_j})\}_{j=1}^\infty$ is a convergent subsequence of $\{(\boldsymbol{\theta}^t, \boldsymbol{\beta}^t)\}_{t=1}^\infty$ with limit $(\boldsymbol{\theta}^*, \boldsymbol{\beta}^*)$. Then $(\boldsymbol{\theta}^*, \boldsymbol{\beta}^*)$ is a stationary point of (2): $(\boldsymbol{\theta}^*, \boldsymbol{\beta}^*)$ is feasible for (2) and there exists $\psi^* \in \mathbf{R}$ and $\mathbf{v}^* \in \mathbf{R}^{k-1}$ such that $\mathbf{0} \in \partial L(\boldsymbol{\theta}^*, \boldsymbol{\beta}^*, \psi^*, \mathbf{v}^*)$, where $\partial L(\boldsymbol{\theta}, \boldsymbol{\beta}, \psi, \mathbf{v})$ denotes the subdifferential of the Lagrangian function L with respect to the primal variables $(\boldsymbol{\theta}, \boldsymbol{\beta})$.*

A proof of Theorem 2.5 can be found in Appendix C.

3 Numerical Simulations

We next compare the performance of our proposed approaches with standard methods for penalized discriminant analysis in several numerical experiments. In particular, we compare the implementations of the block coordinate descent method Algorithm 1, where each discriminant direction $\boldsymbol{\beta}$ is updated using either the proximal gradient method with constant step size, Algorithm 3 (PG), the proximal gradient method with backtracking line search, Algorithm 2 (PGB), the accelerated proximal method with constant step size, Algorithm 4 (APG), the accelerated proximal method with backtracking, Algorithm 5 (APGB), and the alternating direction method of multipliers, Algorithm 6, (ADMM), with the least angle regression based algorithm for solving the sparse optimal scoring problem proposed in [10]. All simulations were conducted using R version 3.5.0 and our heuristics are implemented in R as the package **accSDA** (see [12]). The all runs were performed on a standard node of the University of Alabama's research computing cluster (UAHPC).

3.1 Classification of Spectral and Time Series Data

We first apply each of these methods to learn classification rules for the following data sets: the *Penicillium* (*Pen*) data set from [9] of multi-spectral images of three *Penicillium* species that are almost visually indistinguishable ($p = 3542, K = 3$ training sample size = 24, testing sample size = 12); *Electrocardiogram measurements* (*ECG*) of a 67-year old male taken on two dates, five days apart, before and after corrective cardiac surgery ($p = 136, K = 2$, training size = 23, testing size = 861); food spectrogram observations of either Arabica or Robusta variants of instant coffee ($p = 286, K = 2$, training size = 28, testing size = 28); food spectrogram observations of extra virgin olive oil originating from one of four countries ($p = 570, K = 4$, training size = 30, testing size = 30). The final three data sets were obtained from the UC Riverside classification data repository [8]. We use each heuristic to obtain $q = K - 1$ sparse discriminant vectors and

Table 2: Summary of classification performance of benchmarking data using nearest centroid classification and the sparse zero variance method (SZVD) or sparse optimal scoring vectors calculated using the proximal gradient method with constant stepsize (PG), with backtracking line search (PGB), accelerated proximal method with constant stepsize (APG) and backtracking line search (APGB), alternating direction method of multipliers (ADMM), and least angle regression (LARS). Each block reports the four best methods in terms of number of classification errors on out-of-sample testing observations (numErr), fraction of nonzero features (fracFeat), and time (in seconds) needed to train the discriminant vectors (runTime). Ties are indicated by “*”. To highlight improvement over the LARS algorithm, we report the value of each statistic for the LARS algorithm and the ranking of LARS with respect to each statistics in the form Value (Rank) in the LV(R) rows of the table.

Dataset	numErr		fracFeat		runTime	
Pen	1st*	PG 0.00e+00	1st	APGB 3.42e-02	1st	APG 4.05e+01
p=3542	1st*	PGB 0.00e+00	2nd	APG 3.98e-02	2nd	APGB 1.54e+02
K=3	1st*	APG 0.00e+00	3rd	PG 4.73e-02	3rd	PG 4.16e+02
ntrain=24	1st*	APGB 0.00e+00	4th	PGB 4.74e-02	4th	ADMM 5.94e+02
ntest=12	LV(R)	1.00e+00 (2)	LV(R)	5.05e-02 (5)	LV(R)	4.35e+04 (7)
ECG	1st	ADMM 1.80e+01	1st	LARS 2.94e-02	1st	SZVD 2.32e+00
p=136	2nd	SZVD 2.40e+01	2nd	APG 7.35e-02	2nd	LARS 2.70e+00
K=2	3rd	PGB 3.50e+01	3rd	APGB 8.82e-02	3rd	APG 4.05e+00
ntrain=23	4th	APGB 8.10e+01	4th	PG 1.10e-01	4th	PG 1.03e+01
ntest=861	LV(R)	1.30e+02 (7)	LV(R)	2.94e-02 (1)	LV(R)	2.70e+00 (2)
Coffee	1st*	PG 0.00e+00	1st	LARS 2.80e-02	1st	LARS 7.48e+00
p=286	1st*	PGB 0.00e+00	2nd*	PG 1.15e-01	2nd	APG 8.52e+00
K=2	1st*	APG 0.00e+00	2nd*	PGB 1.15e-01	3rd	SZVD 1.38e+01
ntrain=28	1st*	APGB 0.00e+00	3rd	APG 1.22e-01	4th	APGB 3.71e+01
ntest=28	LV(R)	0.00e+00 (1*)	LV(R)	2.80e-02 (1)	LV(R)	7.48e+00 (1)
Olive Oil	1st*	ADMM 1.00e+00	1st	APG 1.19e-01	1st	APG 8.20e+01
p=570	1st*	SZVD 1.00e+00	2nd	APGB 1.26e-01	2nd	APGB 3.44e+02
K=4	1st*	LARS 1.00e+00	3rd	PGB 1.61e-01	3rd	PG 4.48e+02
ntrain=30	2nd*	PG 2.00e+00	4th*	PG 1.93e-01	4th	ADMM 5.29e+02
ntest=30	LV(R)	1.00e+00 (1*)	LV(R)	1.93e-01 (4*)	LV(R)	1.02e+03 (6)

then perform nearest-centroid classification after projection onto the subspace spanned by these discriminant directions. The results of our experiments are summarized in Table 2 and Figure 1. Full results from these experiments can be found in Table 5 found in Appendix D.

The sparse discriminant analysis heuristics require training of the regularization parameters γ , $\mathbf{\Omega}$, and λ . In all experiments, we set $\gamma = 10^{-3}$ and $\mathbf{\Omega}$ to be the $p \times p$ identity matrix $\mathbf{\Omega} = \mathbf{I}$. We train the remaining parameter λ using N -fold cross validation. Specifically, we choose λ from a set of potential λ of the form $\bar{\lambda}/2^c$ for $c = 9, 8, 7, \dots, -1, -2, -3$ and $\bar{\lambda}$ chosen so that the problem has nontrivial solution for all considered λ . Note that (10) has optimal solution given by $\beta^* = \mathbf{A}^{-1}\mathbf{d}$ if we set $\lambda = 0$; this implies that choosing

$$\bar{\lambda} = \frac{(\beta^*)^T \mathbf{d} - \frac{1}{2}(\beta^*)^T \mathbf{A} \beta^*}{\|\beta^*\|_1} \quad (23)$$

ensures that there exists at least one solution β^* with value strictly less than zero. We choose the value of λ with fewest average number of misclassification errors over training-validation splits amongst all λ which yield discriminant vectors containing at most 15% nonzero entries. The LARS algorithm terminates after a solution with desired maximum cardinality is identified; we apply N -fold cross validation to select this maximum cardinality from 13 equally spaced potential values from $0.025qp$ to $0.5qp$. We set the number

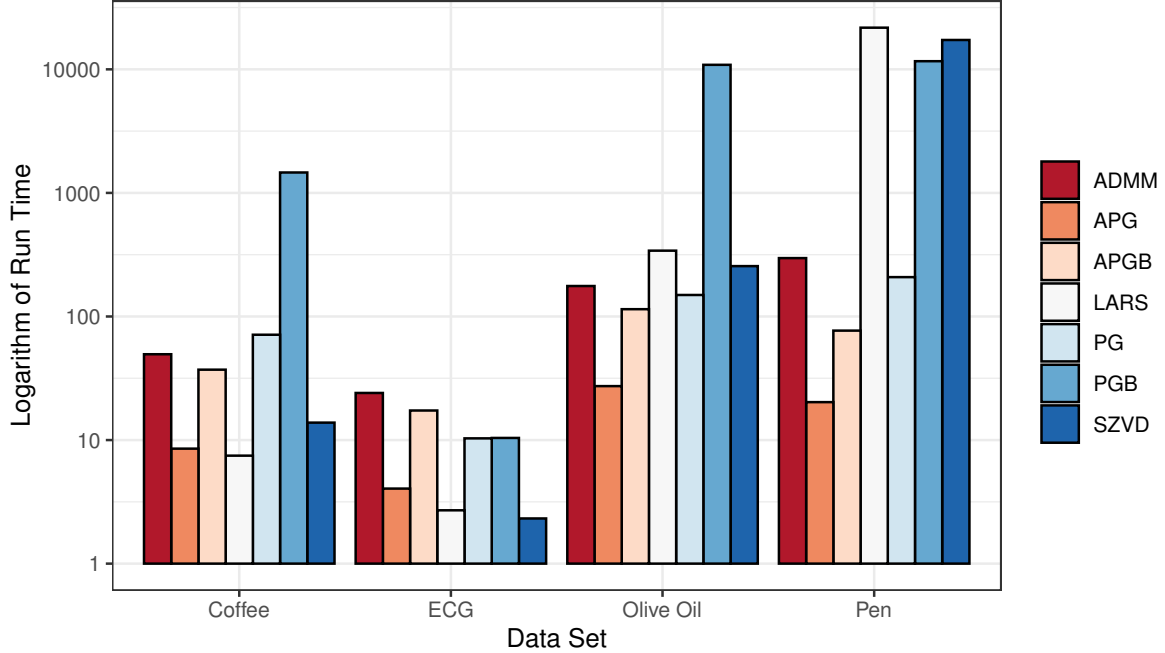


Figure 1: Logarithm of run times for penalized linear discriminant analysis heuristics: proximal gradient method with constant stepsize (PG), with backtracking line search (PGB), accelerated proximal method with constant stepsize (APG) and backtracking line search (APGB), alternating direction method of multipliers (ADMM), least angle regression (LARS) (all for sparse optimal scoring) and sparse zero variance discriminant analysis (SZVD). Reported values are the logarithm of the ratio of total run time divided by the number of discriminant vectors calculated ($q = K - 1$).

of folds $N = 5, 5, 7, 15$ for the *Pen*, *ECG*, *Coffee*, and *Olive oil* data sets respectively. We terminate each proximal algorithm in the inner loop after 1000 iterations or a 10^{-5} suboptimal solution is obtained; the outer block coordinate descent loop is stopped after a maximum number of 250 iterations or a 10^{-3} suboptimal solution has been found. The augmented Lagrangian parameter $\mu = 5$ was used in all experiments in the ADMM method (SDAD). We use the value of $\bar{L} = 0.25$ for the initial estimate of the Lipschitz constant and $\eta = 1.25$ for the scalar multiplier in the backtracking line search.

We also include the Sparse Zero Variance Discriminant Analysis (SZVD) method proposed in [2] in our comparisons. We train the regularization parameter γ in SZVD in a fashion similar to that above. We set the maximum value of the regularization parameter γ to be $\bar{\gamma} \hat{\beta}^T \mathbf{B} \hat{\beta} / \|\hat{\beta}\|_1$, where $\hat{\beta}$ is the optimal solution of the unpenalized SZVD problem and \mathbf{B} is the sample between-class covariance matrix of the training data. We choose γ from the exponentially spaced grid $\bar{\gamma}/2^c$ for $c = 9, 8, \dots, -2, -3$ using N -fold cross-validation; this approach is consistent with that in [2]. The number of folds N for each data set was identical to that in the SOS cross validation scheme described above. We select the value of γ which minimizes misclassification error amongst all sets of discriminant vectors with at most 35% nonzero entries; this acceptable sparsity threshold is chosen to be higher than that in the SOS experiments, due to the tendency of SZVD to misconverge to the trivial all-zero solution for large values of γ . We stop SZVD after a maximum of 1000 iterations or a solution satisfying the stopping tolerance of 10^{-5} is obtained. We use the augmented Lagrangian penalty parameter $\beta = 5$ in SZVD in all experiments.

Figure 1 clearly illustrates significant computational improvement of using the accelerated proximal gradient and ADMM over the classical LARS method when the number of features is large; APG terminates in approximately 40 seconds when preparing classifiers for the *Pen* data set, while LARS requires over 12 hours. However, when p is relatively small, as it is in all other experiments, we see that the run times of APG and ADMM are similar to that of LARS. We'll discuss this phenomena in greater detail in the next sections.

3.2 Gaussian data

We performed similar simulations investigating efficacy of our heuristics for classification of Gaussian data. In each experiment, we generate data consisting of p -dimensional vectors from one of K multivariate normal distributions. Specifically, we obtain training observations corresponding to the i th class, $i = 1, 2, \dots, K$, by sampling 25 observations from the multivariate normal distribution with mean $\boldsymbol{\mu}_i \in \mathbf{R}^p$ satisfying

$$[\boldsymbol{\mu}_i]_j = \begin{cases} 0.7, & \text{if } 100(i-1) < j \leq 100i \\ 0, & \text{otherwise,} \end{cases} \quad (24)$$

for all $j = 1, 2, \dots, p$, and covariance matrix $\boldsymbol{\Sigma} \in \mathbf{R}^{p \times p}$ chosen so that all features are correlated with $\Sigma_{ij} = r$ for all $i \neq j$ and $\Sigma_{ii} = 1$ for all i . We conduct the experiment for all $K \in \{2, 4\}$, $r \in \{0, 0.1, 0.5, 0.9\}$. For each experiment, we sample 250 testing observations from each class in the same manner as the training data. We set $p = 500$ in each simulation.

For each (K, r) pair we generate 20 data sets and use nearest centroid classification following projection onto the span of the discriminant directions calculated using Algorithm 1 and PG, PGB, APG, APGB, ADMM, or LARS to solve (5), or SZVD. We train any regularization parameters for the SOS and SZVD problems in the same fashion as in Section 3.1 using 5-fold cross validation; we set the desired maximum fraction of nonzero features to 0.35 in the cross validation scheme. We use augmented Lagrangian parameters $\mu = 2$ and $\beta = 5$ in the alternating direction methods Algorithm 6 and SZVD respectively. Otherwise all input parameters were chosen as in Section 3.1. Table 3 summarizes the results of these experiments; full numerical results can be found in Appendix D.

In these simulations, we see that the classical implementation using LARS tends to use fewer predictor variables than the proximal methods and SZVD for binary classification and when there is relatively low correlation between variables, often at a cost of significantly lower prediction accuracy. In this case, LARS has run time similar to that of the proposed proximal methods since the number of flops required by LARS scales with the number of nonzero predictor variables, and not the ambient dimension. When the data contains four classes or with more correlation between variables, the proposed algorithms are much faster than LARS, with significantly fewer classification errors. We further investigate this phenomena in the following sections.

3.3 Convergence Experiments

The empirical results of Sections 3.1 and 3.2 suggest that the use of our proposed proximal methods (PG, PGB, APG, APGB, ADMM) for solution of the (5) can lead to significant improvement in terms of classification accuracy and overall run time over the least angle regression algorithm. To further illustrate this improvement, we performed a series of experiments investigating the behaviour of the objective function of (2) during each iteration of these methods.

We call Algorithm 1 to perform nearest centroid classification to each of the *Coffee* and *ECG* data sets using the proximal gradient method with back tracking line search (PGB) and with constant step length (PG), the accelerated gradient method with and without back tracking (APGB, APG, respectively), alternating direction method of multipliers (ADMM), and least angle regression (LARS) to solve (5). We set the number of subproblem iterations to be equal to 10000, stopping tolerance for the subproblem to be $10^{-5}/\sqrt{p}$, and use regularization parameters $\gamma = 10^{-3}$, $\boldsymbol{\Omega} = \mathbf{I}$. We set $\lambda = 0.05\bar{\lambda}$, where $\bar{\lambda}$ is given by (23); we stop LARS when a solution with cardinality matching the maximum cardinality of all other methods is found. We use augmented Lagrangian parameter $\mu = 2$ in ADMM. We use the parameters $\bar{L} = 0.25$ and $\eta = 1.25$ in the back tracking line search. We repeated the process 100 times for each method and data set to control for natural variation in computation time; each algorithms will generate the same sequence of iterates and solution each time (up to sign changes due to random initialization of $\boldsymbol{\theta}$).

We also generated 100 random data sets with observations sampled from one of two normal distributions, $N(\boldsymbol{\mu}_1, \boldsymbol{\Sigma})$ or $N(\boldsymbol{\mu}_2, \boldsymbol{\Sigma})$. Specifically, we sampled $n = 200$ training observations from each of the p -dimensional multivariate Gaussian distributions for $p = 2000$ with mean vectors $\boldsymbol{\mu}_1$ and $\boldsymbol{\mu}_2 \in \mathbf{R}^p$, respectively, satisfying

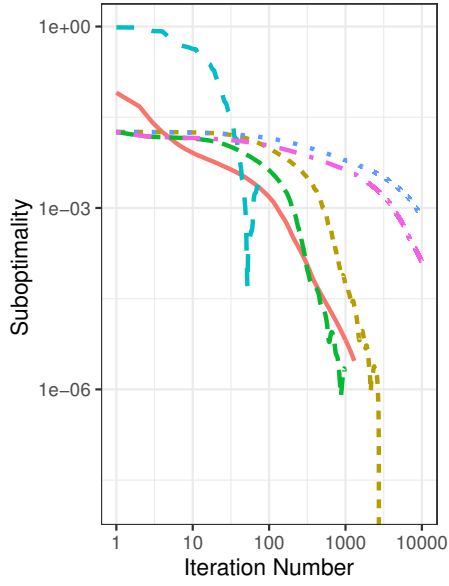
$$[\boldsymbol{\mu}_i]_j = \begin{cases} 0.7, & \text{if } \lceil p/3 \rceil (i-1) < j \leq \lceil p/3 \rceil i \\ 0, & \text{otherwise,} \end{cases} \quad (25)$$

Table 3: Summary of classification performance for synthetic data using nearest centroid classification and the sparse zero variance method (SZVD) or sparse optimal scoring vectors calculated using the proximal gradient method with constant stepsize (PG), with backtracking line search (PGB), accelerated proximal method with constant stepsize (APG) and backtracking line search (APGB), alternating direction method of multipliers (ADMM), and least angle regression (LARS). All results are listed in the format “mean (standard deviation)”. Ties are indicated by “*”. In all experiments, $n_{train} = 25K$ and $n_{test} = 250K$. To highlight improvement over the LARS algorithm, we report the value of each statistic for the LARS algorithm and the ranking of LARS with respect to each statistics in the form Value (Rank) in the LV(R) rows of the table.

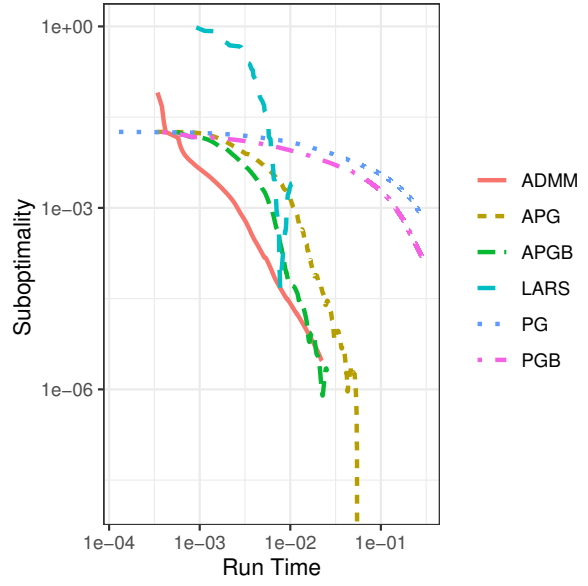
Dataset	numErr		fracFeat		runTime	
p=500 r=0 K=2	1st	ADMM 0.00e+00 (0.00e+00)	1st	LARS 2.60e-02 (0.00e+00)	1st	APG 2.96e+00 (2.53e-01)
	2nd	SZVD 1.00e-01 (3.16e-01)	2nd	PGB 2.45e-01 (8.90e-02)	2nd	PG 5.08e+00 (7.19e-01)
	3rd*	PG 6.00e-01 (1.07e+00)	3rd	APGB 2.46e-01 (2.17e-02)	3rd	LARS 1.73e+01 (6.24e-01)
	3rd*	APG 6.00e-01 (5.16e-01)	4th	PG 2.65e-01 (6.74e-02)	4th	APGB 2.86e+01 (2.46e+00)
	LV(R)	9.13e+01 (1.66e+01) (6)	LV(R)	2.60e-02 (0.00e+00) (1)	LV(R)	1.73e+01 (6.24e-01) (3)
p=500 r=0.1 K=2	1st	ADMM 0.00e+00 (0.00e+00)	1st	LARS 2.60e-02 (0.00e+00)	1st	APG 3.24e+00 (1.38e-01)
	2nd	SZVD 1.00e-01 (3.16e-01)	2nd	PGB 2.36e-01 (7.69e-02)	2nd	PG 5.73e+00 (6.16e-01)
	3rd	APG 4.00e-01 (5.16e-01)	3rd	PG 2.82e-01 (6.41e-02)	3rd	LARS 1.71e+01 (6.46e-01)
	4th	PG 5.00e-01 (8.50e-01)	4th	SZVD 3.30e-01 (1.48e-02)	4th	APGB 2.88e+01 (2.23e+00)
	LV(R)	9.13e+01 (1.70e+01) (7)	LV(R)	2.60e-02 (0.00e+00) (1)	LV(R)	1.71e+01 (6.46e-01) (3)
p=500 r=0.5 K=2	1st*	PGB 0.00e+00 (0.00e+00)	1st	LARS 2.60e-02 (0.00e+00)	1st	APG 4.86e+00 (4.29e-01)
	1st*	APG 0.00e+00 (0.00e+00)	2nd	PGB 2.32e-01 (4.67e-02)	2nd	PG 1.63e+01 (1.86e+00)
	1st*	APGB 0.00e+00 (0.00e+00)	3rd	PG 2.34e-01 (6.80e-02)	3rd	LARS 1.90e+01 (7.45e-01)
	1st*	ADMM 0.00e+00 (0.00e+00)	4th	SZVD 3.50e-01 (1.65e-02)	4th	APGB 3.17e+01 (1.09e+00)
	LV(R)	5.48e+01 (2.02e+01) (3)	LV(R)	2.60e-02 (0.00e+00) (1)	LV(R)	1.90e+01 (7.45e-01) (3)
p=500 r=0.9 K=2	1st*	PG 0.00e+00 (0.00e+00)	1st	LARS 2.60e-02 (0.00e+00)	1st	APG 3.99e+00 (3.69e-01)
	1st*	PGB 0.00e+00 (0.00e+00)	2nd	APG 1.85e-01 (3.80e-02)	2nd	PG 1.95e+01 (2.73e+00)
	1st*	APG 0.00e+00 (0.00e+00)	3rd	PGB 2.14e-01 (7.59e-02)	3rd	LARS 2.03e+01 (1.27e+00)
	1st*	APGB 0.00e+00 (0.00e+00)	4th	APGB 2.29e-01 (5.46e-02)	4th	APGB 2.44e+01 (1.71e+00)
	LV(R)	3.40e+00 (5.30e+00) (2)	LV(R)	2.60e-02 (0.00e+00) (1)	LV(R)	2.03e+01 (1.27e+00) (3)
p=500 r=0 K=4	1st	SZVD 2.90e+00 (1.37e+00)	1st	LARS 2.22e-01 (4.16e-03)	1st	PG 1.33e+01 (9.68e-01)
	2nd	ADMM 5.90e+00 (5.69e+00)	2nd	APG 5.64e-01 (1.19e-01)	2nd	APG 1.47e+01 (6.24e-01)
	3rd	PG 1.50e+01 (1.13e+01)	3rd	PG 5.85e-01 (1.42e-01)	3rd	APGB 1.86e+02 (5.66e+00)
	4th	PGB 1.83e+01 (1.59e+01)	4th	PGB 5.89e-01 (1.58e-01)	4th	SZVD 2.05e+02 (8.80e+00)
	LV(R)	1.01e+02 (9.91e+00) (7)	LV(R)	2.22e-01 (4.16e-03) (1)	LV(R)	3.61e+02 (2.25e+01) (6)
p=500 r=0.1 K=4	1st	SZVD 2.00e+00 (1.89e+00)	1st	LARS 2.21e-01 (4.02e-03)	1st	PG 1.50e+01 (1.09e+00)
	2nd	ADMM 4.30e+00 (3.33e+00)	2nd	PGB 5.02e-01 (7.52e-02)	2nd	APG 1.61e+01 (6.12e-01)
	3rd	PG 1.81e+01 (1.99e+01)	3rd	APG 5.28e-01 (9.06e-02)	3rd	APGB 1.83e+02 (6.60e+00)
	4th	APG 2.90e+01 (1.35e+01)	4th	APGB 5.85e-01 (6.68e-02)	4th	SZVD 2.07e+02 (5.57e+00)
	LV(R)	1.49e+02 (1.25e+01) (7)	LV(R)	2.21e-01 (4.02e-03) (1)	LV(R)	3.69e+02 (1.41e+01) (6)
p=500 r=0.5 K=4	1st	ADMM 4.00e-01 (1.26e+00)	1st	LARS 2.16e-01 (3.33e-03)	1st	APG 2.23e+01 (1.72e+00)
	2nd	SZVD 1.00e+00 (3.16e+00)	2nd	PG 4.94e-01 (4.32e-02)	2nd	PG 4.57e+01 (5.82e+00)
	3rd	APG 2.60e+00 (2.27e+00)	3rd	PGB 5.02e-01 (2.52e-02)	3rd	APGB 1.83e+02 (6.03e+00)
	4th	PGB 3.20e+00 (2.90e+00)	4th	APG 5.13e-01 (2.21e-02)	4th	SZVD 2.06e+02 (8.72e+00)
	LV(R)	5.77e+01 (1.20e+01) (7)	LV(R)	2.16e-01 (3.33e-03) (1)	LV(R)	3.63e+02 (2.25e+01) (6)
p=500 r=0.9 K=4	1st*	ADMM 0.00e+00 (0.00e+00)	1st	LARS 7.61e-02 (2.11e-04)	1st	APG 2.05e+01 (1.16e+00)
	1st*	SZVD 0.00e+00 (0.00e+00)	2nd	APG 1.27e-01 (2.60e-02)	2nd	PG 5.74e+01 (6.05e+00)
	2nd	LARS 2.00e-01 (4.22e-01)	3rd	PGB 1.46e-01 (7.53e-02)	3rd	APGB 1.60e+02 (5.83e+00)
	3rd	APGB 1.00e+00 (1.63e+00)	4th	APGB 1.51e-01 (4.67e-02)	4th	SZVD 2.09e+02 (4.42e+00)
	LV(R)	2.00e-01 (4.22e-01) (2)	LV(R)	7.61e-02 (2.11e-04) (1)	LV(R)	3.86e+02 (1.76e+01) (6)

for all $j = 1, 2, \dots, p$, and covariance matrix $\Sigma \in \mathbf{R}^{p \times p}$ constructed as Section 3.2 with $r = 0.75$. For each data set, we train nearest centroid classifiers using discriminant vectors obtained by approximately solving (2) with each method used above (PG, PGB, APG, APGB, ADMM, LARS) to solve (5). We stop each method after either 2500 iterations have been performed or the stopping condition is met with tolerance $10^{-4}/\sqrt{p}$; otherwise all inputs are consistent with those used for the *Coffee* and *ECG* data. We validate performance of our classifiers using balanced sets of 200 testing observations sampled from $N(\mu_1, \Sigma)$ or $N(\mu_2, \Sigma)$.

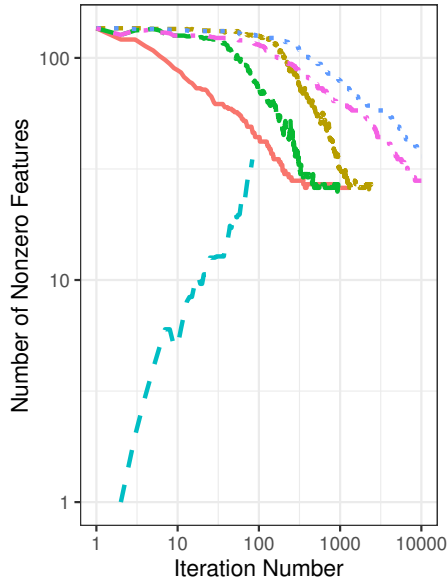
We chose these data sets to isolate the relationship between the performance of our proposed algorithms



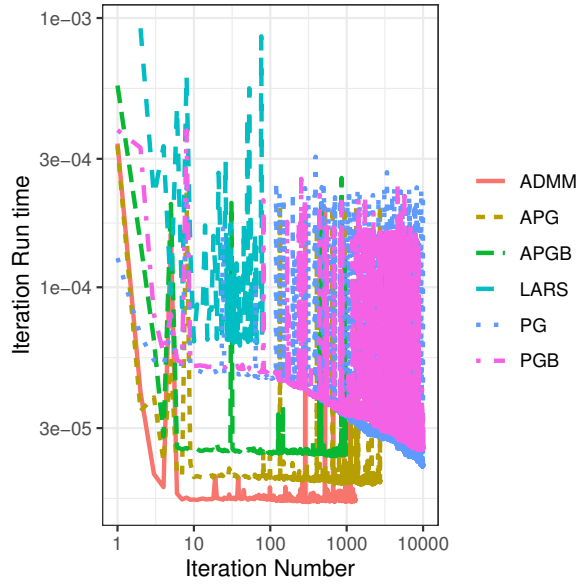
(a) Value (w.r.t. iteration)



(b) Value (w.r.t. run time)

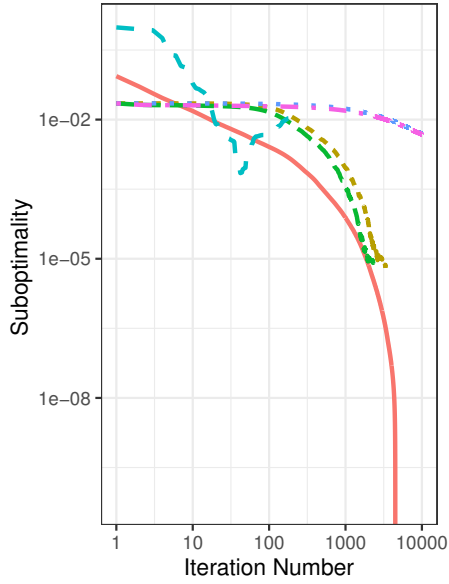


(c) Cardinality (w.r.t. iteration)

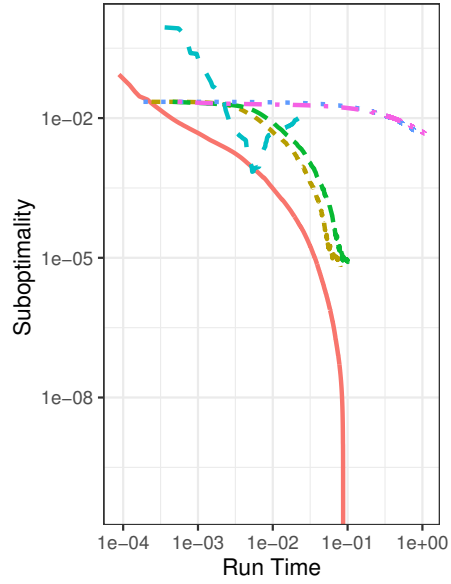


(d) Iteration run time

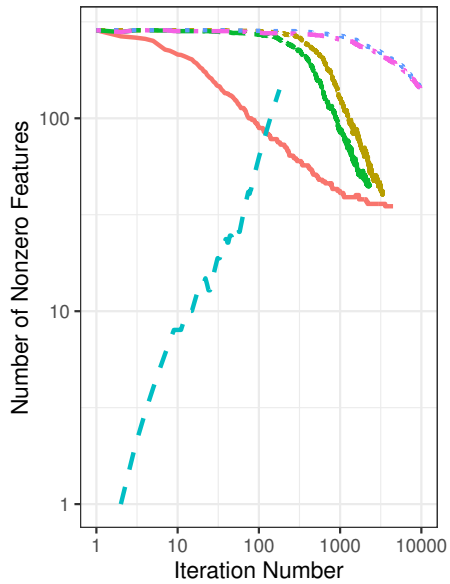
Figure 2: Objective value (with respect to iteration number and run time so far), cardinality of iterate, and iteration run time for *ECG* data set.



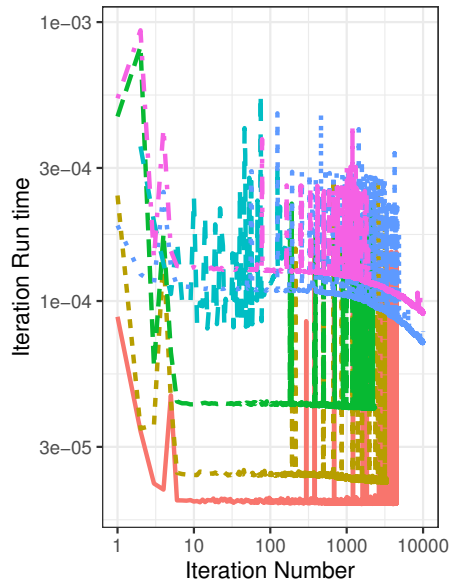
(a) Value (w.r.t. iteration)



(b) Value (w.r.t. run time)



(c) Cardinality (w.r.t. iteration)



(d) Iteration run time

Figure 3: Objective value (with respect to iteration number and run time so far), cardinality of iterate, and iteration run time for *Coffee* data set.

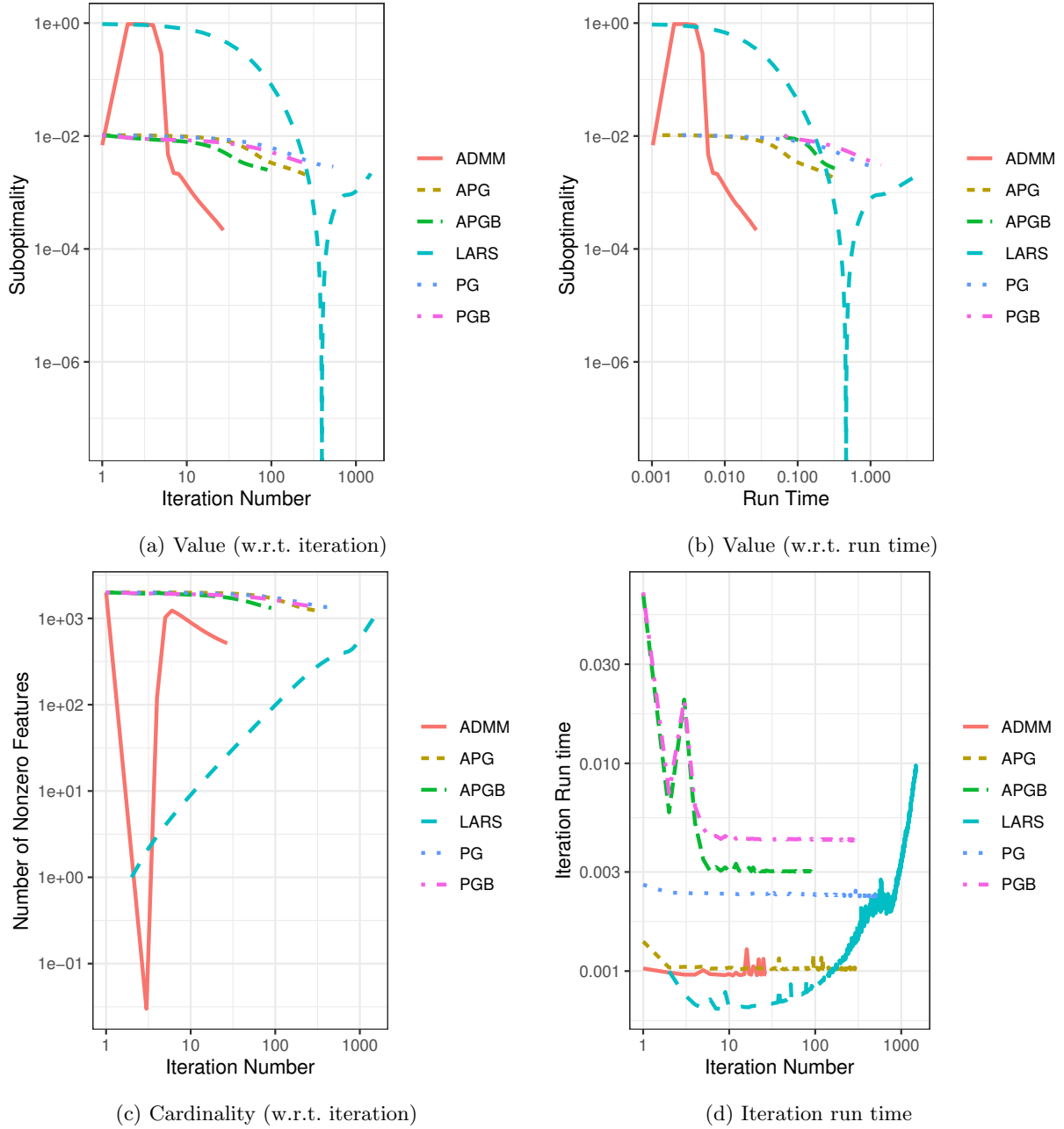
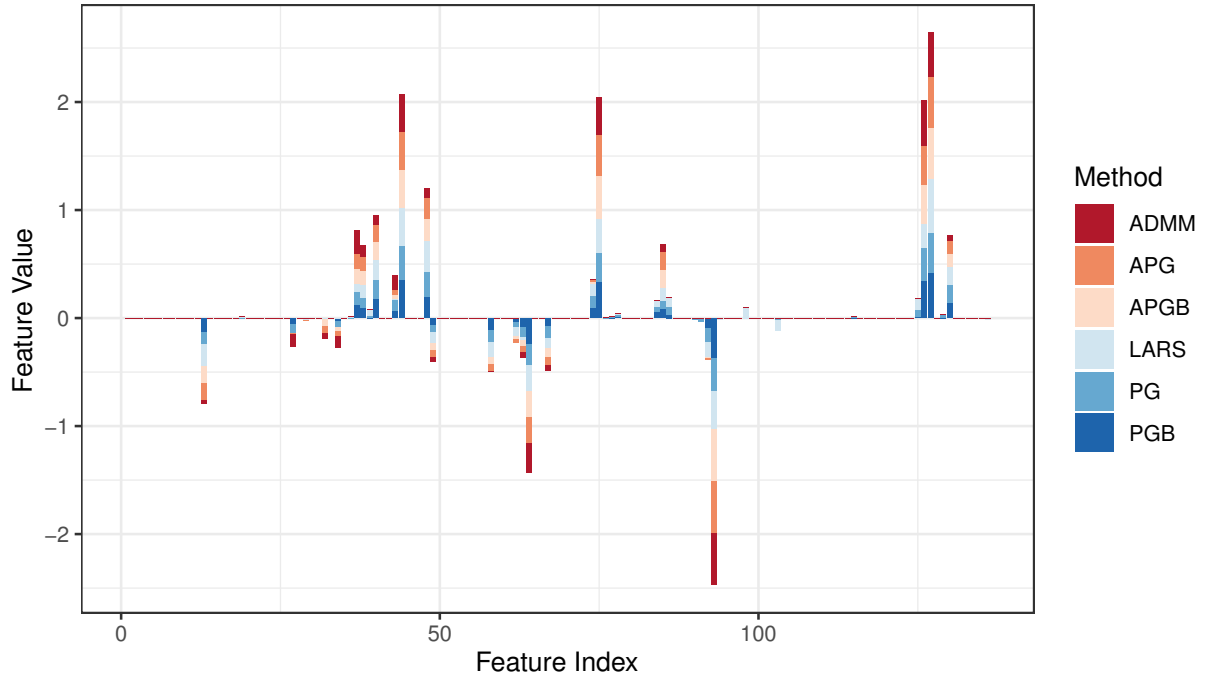
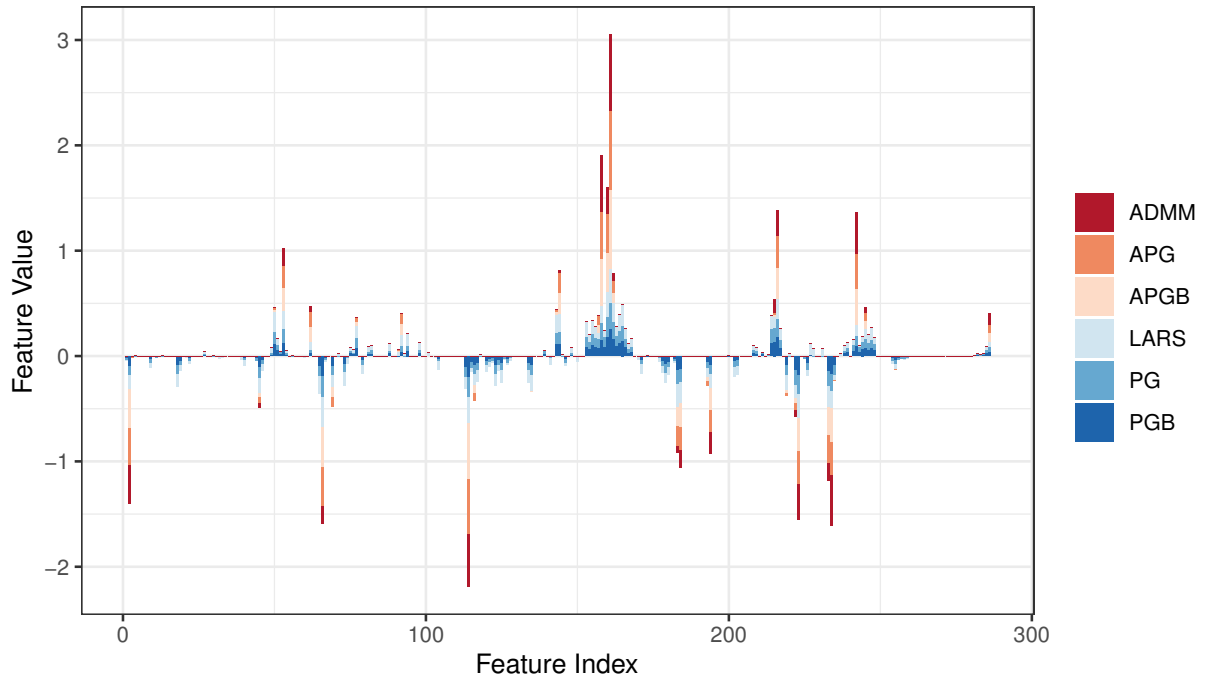


Figure 4: Objective value (with respect to iteration number and run time so far), cardinality of iterate, and iteration run time averaged over 100 Gaussian data sets.



(a) *ECG*



(b) *Coffee*

Figure 5: Discriminant vectors for *ECG* and *Coffee* data sets. We stack the bars representing the value of the entry of each discriminant vector calculated by each method to ease legibility of the bar plot. The discriminant vectors returned by each method share roughly the same sparsity pattern, with ADMM most sparse and PG/PGB most dense.

for solving (5) and the overall performance of the proposed block coordinate descent method and nearest centroid classification. In the $K = 2$ class case, we calculate exactly one discriminant and scoring vector pair (β, θ) . Consequently, we expect the block coordinate descent method to converge after exactly one full iteration in the absence of rounding error. Indeed, the optimal solution of (3) is given by the projection of any vector θ not in the span of the all-ones vector \mathbf{e} onto the set of all $\theta \in \mathbf{R}^K$ satisfying $\theta^T \mathbf{Y}^T \mathbf{Y} \theta = n$ and $\theta^T \mathbf{Y}^T \mathbf{Y} \mathbf{e} = 0$; this is equivalent to the optimal solution given by Lemma 2.1. This solution is uniquely defined (up to sign) and is obtained after the initial θ update if the initial solution θ is not a scalar multiple of \mathbf{e} . This suggests that Algorithm 1 will converge after exactly one iteration if we solve (5) exactly. In practice, we may require multiple iterations of Algorithm 1 depending on the relative stopping tolerances of Algorithm 1 and the method used to solve (5); we terminate the block coordinate descent method after one iteration in these experiments.

We recorded the objective value of (5) and the cardinality of the current iterate β^t following the t th iteration of each algorithm for each method and data set, as well as the run time of the t th iteration. We recorded the value of the augmented Lagrangian function for the ADMM, instead of the objective function value, to indicate the trade-off between optimizing the objective and forcing feasibility ($\mathbf{x} = \mathbf{y} = \beta$) of the split decision variables \mathbf{x} and \mathbf{y} . We also recorded the cardinality and number of misclassification errors of each scoring and discriminant vector pairs calculated by each method. The results of these experiments are summarized in Figures 2, 3, and 4 and Table 4. All experiments were conducted on the UAHPC using Matlab 2019a.

It is apparent from the results of these simulations that iterations of LARS are significantly more expensive than those of the proximal methods, particularly, when the cardinality of the iterate is relatively large. The per-iteration cost of LARS tends to increase as a function of iteration number due to the corresponding increase in cardinality each iteration. Since LARS is an active set method and gradually adds elements to the active set each iteration, we see that LARS terminates earliest when the dimension p is smallest. In this case, both total number of iterations and per-iteration cost is minimized, making LARS an appealing method in such situations; see Figure 2 and the section of Table 4 regarding the *ECG* data set, where LARS features significantly more expensive iterations than the proximal methods but uses less computation time than all but ADMM overall, since it terminates in much fewer iterations than the other methods. However, when p is large the increased per-iteration cost (for later iterations) and increased total number of iterations performed causes LARS to be less efficient than the proximal methods in terms of overall computational complexity.

On the other hand, the per-iteration cost of each proximal method is largely consistent across iterations. The ADMM tended to terminate in fewer iterations and yield sparser solutions than the other proximal methods; the per-iteration cost of the ADMM is also less than (or comparable to) the other proximal methods in all trials. The cardinality of iterates generated by ADMM also decreased much more quickly than those generated by the other proximal methods; this is may be due to the fact that the soft thresholding operator is applied directly to the iterate \mathbf{y}^t , rather than following a gradient step applied to the previous iterate or a weighted average of the previous two iterates as in the proximal gradient and accelerated gradient methods.

These trials also suggest some modest value in the use of back tracking line searches. In each set of trials, the proximal gradient methods with back tracking line search terminated in fewer iterations than with a constant step size; we should note that the proximal gradient method does not terminate within 10000 iterations for both the *ECG* and *Coffee* data sets for either choice of step size. However, the additional cost of performing the line search frequently caused the overall computational time of the back tracking methods to often exceed that of the constant step size methods. This additional cost is not as dramatic as those observed in Sections 3.1 and 3.2. We remind the reader that the reported computation time for the experiments of Sections 3.1 and 3.2, includes all computation to perform cross validation to train the regularization parameter λ ; the discrepancy between the timing results in Sections 3.1 and 3.2 and here highlights a potential sensitivity of Algorithm 1 to choice of λ , training data (in this case with respect to training and validation splits in the cross validation scheme), and computing environment (R versus Matlab).

At this point, we should note that in all experiments considered so far, the subproblem (5) is strongly convex by the choice of regularization parameter $\Omega = \mathbf{I}$. As a consequence, (5) has a *unique* solution. One would naively expect Algorithm 1 to generate the same discriminant vector regardless of choice of algorithm for solving (5) if all other input parameters are chosen consistently. However, this is not observed in practice.

Table 4: Results for repeated nearest centroid classification for *Coffee* and *ECG* data sets and Gaussian data sets. All results are listed in the format “mean (standard deviation)”. Bold entries indicate minimum average values for each statistic and data set.

ECG	PG	PGB	APG	APGB	ADMM	LARS
numErr	2.10e+01 (0.00e+00)	2.00e+01 (0.00e+00)	2.33e+01 (4.41e-01)	2.30e+01 (0.00e+00)	2.40e+01 (0.00e+00)	1.80e+01 (0.00e+00)
fracErr	2.44e-02 (0.00e+00)	2.32e-02 (0.00e+00)	2.70e-02 (5.12e-04)	2.67e-02 (0.00e+00)	2.79e-02 (0.00e+00)	2.09e-02 (0.00e+00)
numFeat	3.50e+01 (0.00e+00)	2.80e+01 (0.00e+00)	2.60e+01 (1.00e-01)	2.40e+01 (0.00e+00)	2.60e+01 (0.00e+00)	3.50e+01 (0.00e+00)
fracFeat	2.57e-01 (0.00e+00)	2.06e-01 (0.00e+00)	1.91e-01 (7.35e-04)	1.76e-01 (0.00e+00)	1.91e-01 (0.00e+00)	2.57e-01 (0.00e+00)
runTime	3.64e-01 (9.02e-02)	3.73e-01 (6.75e-02)	7.85e-02 (2.64e-02)	3.43e-02 (2.12e-02)	3.44e-02 (1.82e-02)	1.53e-02 (3.13e-02)
numIts	1.00e+04 (0.00e+00)	1.00e+04 (0.00e+00)	2.80e+03 (8.26e+01)	9.74e+02 (0.00e+00)	1.30e+03 (0.00e+00)	8.30e+01 (0.00e+00)
TimePerIt	3.64e-05 (9.01e-06)	3.72e-05 (6.75e-06)	2.80e-05 (9.68e-06)	3.52e-05 (2.17e-05)	2.64e-05 (1.40e-05)	1.84e-04 (3.78e-04)
Coffee	PG	PGB	APG	APGB	ADMM	LARS
numErr	0.00e+00 (0.00e+00)	0.00e+00 (0.00e+00)	0.00e+00 (0.00e+00)	0.00e+00 (0.00e+00)	0.00e+00 (0.00e+00)	0.00e+00 (0.00e+00)
fracErr	0.00e+00 (0.00e+00)	0.00e+00 (0.00e+00)	0.00e+00 (0.00e+00)	0.00e+00 (0.00e+00)	0.00e+00 (0.00e+00)	0.00e+00 (0.00e+00)
numFeat	1.41e+02 (0.00e+00)	1.37e+02 (0.00e+00)	3.60e+01 (0.00e+00)	3.40e+01 (0.00e+00)	3.50e+01 (0.00e+00)	1.39e+02 (0.00e+00)
fracFeat	4.93e-01 (0.00e+00)	4.79e-01 (0.00e+00)	1.26e-01 (0.00e+00)	1.19e-01 (0.00e+00)	1.22e-01 (0.00e+00)	4.86e-01 (0.00e+00)
runTime	1.10e+00 (1.05e-01)	1.29e+00 (4.17e-02)	1.61e-01 (3.67e-02)	1.67e-01 (3.45e-02)	1.87e-01 (3.23e-02)	2.81e-02 (1.46e-02)
numIts	1.00e+04 (0.00e+00)	1.00e+04 (0.00e+00)	3.49e+03 (4.08e+01)	2.51e+03 (6.34e+01)	4.48e+03 (0.00e+00)	1.79e+02 (0.00e+00)
TimePerIt	1.10e-04 (1.05e-05)	1.29e-04 (4.17e-06)	4.61e-05 (1.05e-05)	6.65e-05 (1.35e-05)	4.18e-05 (7.21e-06)	1.57e-04 (8.13e-05)
Gaussians	PG	PGB	APG	APGB	ADMM	LARS
numErr	0.00e+00 (0.00e+00)	0.00e+00 (0.00e+00)	0.00e+00 (0.00e+00)	0.00e+00 (0.00e+00)	0.00e+00 (0.00e+00)	0.00e+00 (0.00e+00)
fracErr	0.00e+00 (0.00e+00)	0.00e+00 (0.00e+00)	0.00e+00 (0.00e+00)	0.00e+00 (0.00e+00)	0.00e+00 (0.00e+00)	0.00e+00 (0.00e+00)
numFeat	1.13e+03 (2.11e+01)	1.13e+03 (2.11e+01)	5.41e+02 (9.57e+01)	9.45e+02 (1.23e+02)	4.22e+02 (1.43e+01)	9.39e+02 (1.20e+01)
fracFeat	5.67e-01 (1.06e-02)	5.67e-01 (1.06e-02)	2.70e-01 (4.78e-02)	4.72e-01 (6.15e-02)	2.11e-01 (7.15e-03)	4.69e-01 (6.01e-03)
runTime	3.51e+00 (7.24e-01)	4.19e+00 (1.11e+00)	2.40e+00 (4.51e-01)	1.01e+00 (3.13e-01)	2.15e-01 (1.89e-02)	6.34e+00 (1.89e-01)
numIts	7.95e+02 (1.69e+02)	6.39e+02 (1.75e+02)	7.56e+02 (1.48e+02)	1.61e+02 (6.21e+01)	3.00e+01 (1.15e+00)	1.61e+03 (4.06e+01)
TimePerIt	4.42e-03 (4.41e-05)	6.57e-03 (9.15e-05)	3.18e-03 (7.21e-05)	6.38e-03 (4.30e-04)	7.17e-03 (6.24e-04)	3.95e-03 (8.91e-05)

We can see from Figures 2, 3, and 4 that the compared algorithms generate different sequences of iterates whose limit is the unique optimal solution of (5). We terminate each algorithm prematurely at a suboptimal solution, which varies based on our choice of algorithm. Discriminant vectors for the *ECG* and *Coffee* data sets corresponding to the solution of (2) with $\lambda = 0.05\bar{\lambda}$ calculated by Algorithm 1 are plotted in Figure 5; note that the calculated discriminant vectors are qualitatively similar but still differ significantly, particularly in cardinality.

3.4 Scaling Experiments

We next performed a series of simulations to investigate the relationship between performance of our algorithms and the number of features in the underlying data set. Specifically, for each

$$p \in \{250, 300, \dots, 500, 600, \dots, 1000, 1250, \dots, 2500, 3000, \dots, 4500\},$$

we sample 100 data sets, containing two classes drawn from the Gaussian distributions as described in Section 3.2. For each value of p , we sample $\lceil p/10 \rceil$ training and testing observations from each class. Items in the each class are sampled from a multivariate Gaussian distribution with means $\mu_1, \mu_2 \in \mathbf{R}^p$ defined by (25). Both class distributions have covariance matrix Σ having diagonal entries equal to 1 and off-diagonal entries equal to 0.75.

We apply nearest centroid classification following projection onto to the approximate solution of (2) given by the proximal gradient method, accelerated proximal gradient method (with and without backtracking line search) (PG, PGB, APG, APGB), alternating direction method of multipliers (ADMM), and least angle regression method (LARS). We perform exactly one full iteration of the block coordinate descent method (Algorithm 1) for each β -subproblem solver; as before, we should expect Algorithm 1 to terminate after one full iteration, since the optimal choice of θ is obtained in the first iteration (in the absence of numerical error). We choose the regularization parameters in (2) to be $\gamma = 10^{-3}$, $\Omega = \mathbf{I}$, and $\lambda = 0.25\bar{\lambda}$, where $\bar{\lambda}$ is defined as in (23); we used the augmented Lagrangian penalty parameter $\mu = 2$ in ADMM. We terminated the proximal methods when their stopping condition is met with tolerance 10^{-4} or 5000 subproblem iterations have been performed; we used backtracking parameters $\bar{L} = 0.25$ and $\eta = 1.25$ in each run. The LARS heuristic was terminated after a solution was obtained containing the number of nonzero elements of the densest solution returned by the other five methods for each data set. All experiments were conducted on UAHPC using Matlab 2019a.

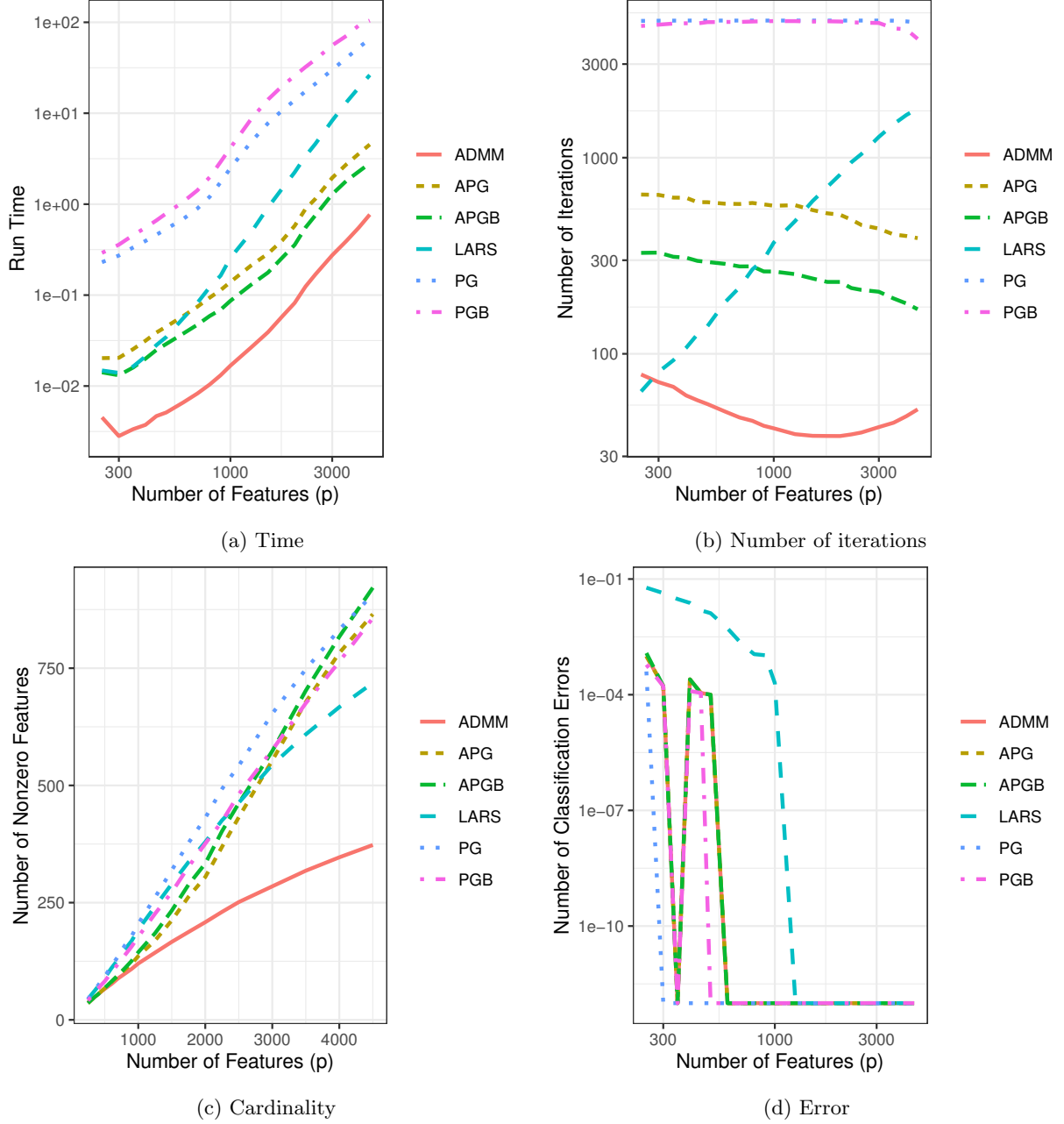


Figure 6: Average run time, number of iterations performed, cardinality of returned solution, and classification error over plotted as a function of number of features p . All axes use logarithmic scale. Misclassification error rates equal to 0 were replaced with 10^{-12} for plotting their logarithm.

Figure 6 summarizes the results of these simulations. We note that the accelerated proximal gradient and alternating direction method of multipliers consistently outperforms the traditional LARS method in terms of run time, number of iterations performed, and classification error. We also note that no methods calculate discriminant vectors which lead to classification error for all $p > 1000$. In particular, these methods require significantly fewer iterations and terminate in less time than LARS for large p . The approximate slopes of the plots of average run times indicate that this phenomena will only be amplified as we increase p further, since the slope of the curve for LARS exceeds that of APG, APGB, and ADMM. This largely agrees with the phenomena predicted by the operation counts discussed in Section 2.4. On the other hand, the proximal gradient methods (PG, PGB) typically do not converge within the maximum number of iterations, which undermines any improvements to computational complexity due to their relatively inexpensive iterations.

We should note that we expect the cardinality of our obtained discriminant vectors increase as a function of p , since the size of the blocks of entries with elevated values in the class-means μ_1 and μ_2 grows linearly with p . This agrees with the plotted curves in Figure 6c. This also explains the linear increase in number of iterations before termination of the LARS method, since the number of iterations depends on the desired number of nonzero entries; in turn, this, along with increase in per-iteration cost as p increases, explains the increase in total run time of LARS as p increases. Finally, the cardinality of returned discriminant vectors scales similarly for the four proximal gradient methods (PG, PGB, APG, APGB) and LARS. The discriminant vectors returned by ADMM consistently contain fewer nonzero entries than the four other methods, which agrees with the behaviour observed in the Section 3.3.

3.5 Multispectral X-ray images and Ω of varying rank

To demonstrate the improvement in run time obtained by using a low-rank Ω in the elastic-net penalty, we perform pixelwise classification on multispectral X-ray images, as presented in [13]. The multispectral X-ray images are scans of food items, where each pixel contains 128 measurements (channels) corresponding to attenuation of X-rays emitted at different wavelengths (see Figure 7). The measurements in each pixel thus give us a profile for the material positioned at that pixel's location (see Figure 8).

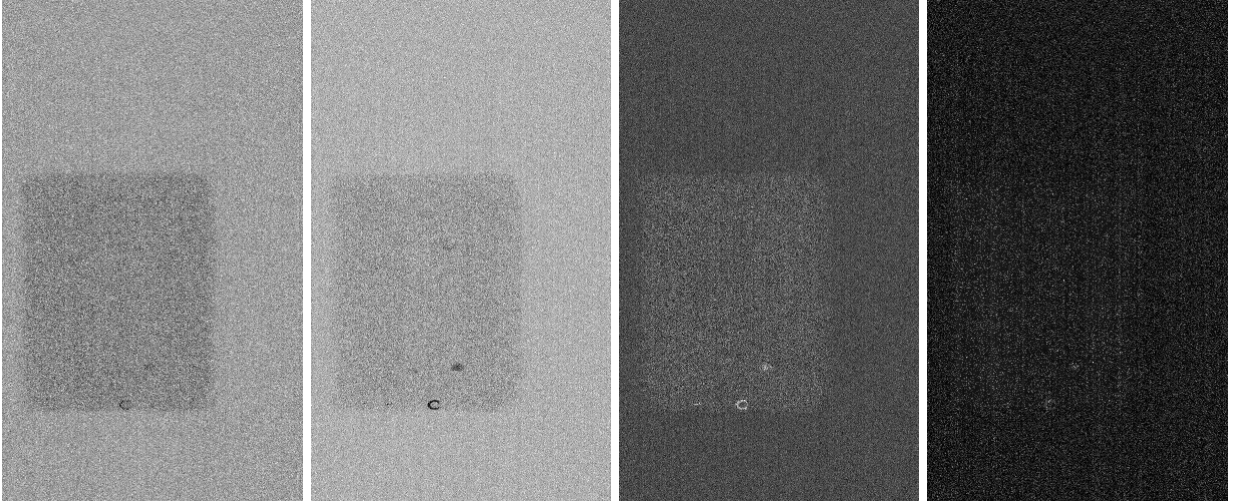


Figure 7: Grayscale images of different channels from a minced meat sample generated with a multispectral X-ray scanner after all preprocessing. From left to right are channels 2, 20, 50 and 100. The contrast decreases the higher we go in the channels and the variation in the measurements increases. Some foreign objects can be seen as small black dots.

We start by preprocessing the scans as in [13] in order to remove scanning artifacts and normalize the intensities between scans. We scale the measurements in each pixel by the 95% quantile of the corresponding 128 measurements instead of the maximum. This scaling approach is more robust in the sense that it is less sensitive to outliers compared to using the maximum. We create our training data by manually selecting rectangular patches from six scans. We have three classes, namely *background*, *minced meat* and *foreign*

Average Material Profiles After Preprocessing

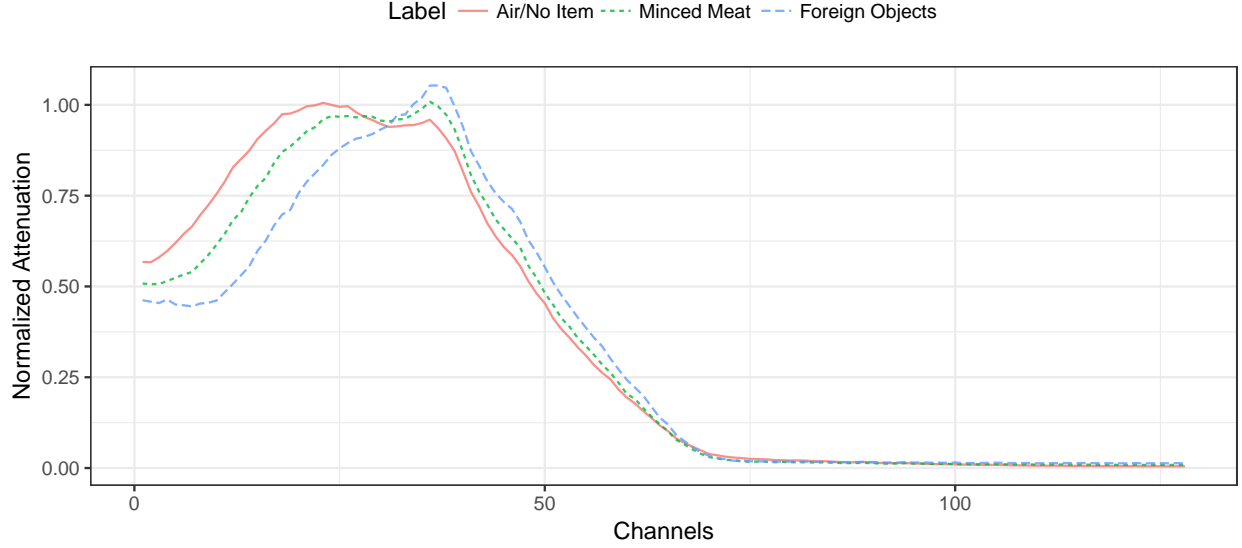


Figure 8: Profiles of materials seen in Figure 7 over the 128 channels. The profile for each type of material, displayed here, is averaged over 500 pixels.

objects. We further subsample the observations to have balanced number of observations, where the class *foreign objects* was under represented. In the end we have 521 observations per class, where each observation corresponds to a single pixel. This data was used to generate Figure 8. For training we use 100 samples per class, and the rest is allocated to a final test set. This process yields 128 variables per observation, but in order to get more spatially consistent classification, we also include data from the pixels located above, to the right, below and to the left of the observed pixel. Thus we have $p = 5 \cdot 128 = 640$ variables per observation. The measurements corresponding to our observation are thus indexed according to spatial and spectral position, i.e., observation \mathbf{x}_i has measurements x_{ijk} , where $j \in \{0, 1, 2, 3, 4\}$ indicates which pixel the measurement belongs to (*center, above, right, bottom, left*), and $k \in \{1, 2, \dots, 128\}$ indicates which channel.

We can impose priors according to these relationships of the measurements in the $\mathbf{\Omega}$ regularization matrix. We assume that the errors should vary smoothly in space and thus impose a Matérn covariance structure on $\mathbf{\Omega}^{-1}$ [25]:

$$C_\nu(d) = \sigma^2 \frac{2^{1-\nu}}{\Gamma(\nu)} \left(\sqrt{2\nu} \frac{d}{\rho} \right)^\nu K_\nu \left(\sqrt{2\nu} \frac{d}{\rho} \right). \quad (26)$$

The Matérn covariance structure (26) is governed by the distance d between measurements. In (26), Γ refers to the gamma function and K_ν is the modified Bessel function of the second kind. For this example we assume that all parameters are 1, except that ν is 0.5. We further assume that the distance between measurements x_{ijk} and $x_{ij'k'}$ from observation i is the Euclidean distance between the points (x_j, y_j, z_k) and $(x_{j'}, y_{j'}, z_{k'})$, where $x_j, y_j, x_{j'}, y_{j'} \in \{-1, 0, 1\}$ and $z_k, z_{k'} \in \{1, 2, \dots, 128\}$. The distance is thus the same as in the image grid (*center, top, bottom, left, right pixel location*), and z -dimension corresponds to the channel.

We use a stopping tolerance of 10^{-5} and a maximum of 1000 iterations for the inner loop using the accelerated proximal algorithm, and a stopping tolerance of 10^{-4} and maximum 1000 iterations for the outer block-coordinate loop. The regularization parameter for the l_1 -norm is selected as $\lambda = 10^{-3}$ and $\gamma = 10^{-1}$ for the Tikhonov regularizer. We present the run time for varying r in Figure 9 and the accuracy with respect to varying r in Figure 10. There is a clear linear trend in rank r for the increase in run time; this agrees with the analysis of Section 2.4. We also estimate the accuracy for a identity regularization matrix, i.e., $\mathbf{\Omega} = \mathbf{I}$, with the same regularization parameters γ and λ and achieve accuracy of 0.948, which is approximately the same accuracy as when using $\mathbf{\Omega}^{400}$. To demonstrate the effect that the rank of $\mathbf{\Omega}$ has on computational complexity, we obtain the singular value decomposition of $\mathbf{\Omega} = \sum_{i=1}^p \sigma_i \mathbf{u}_i \mathbf{v}_i^T$, and construct a low-rank

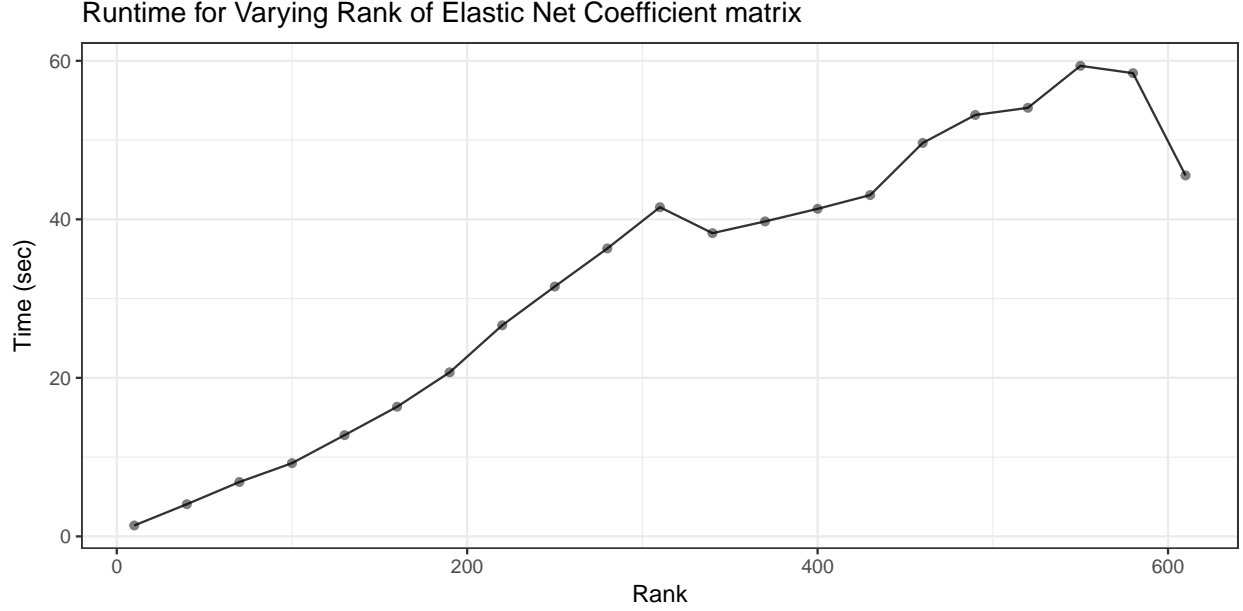


Figure 9: Run time as function of $\text{rank}(\mathbf{\Omega})$. The run time also includes the creation of the low-rank approximated $\mathbf{\Omega}$ matrix.

approximation to $\mathbf{\Omega}$ using the first r singular vectors and singular values: $\mathbf{\Omega}^r = \sum_{i=1}^r \sigma_i \mathbf{u}_i \mathbf{v}_i^T$. We supplied the same parameters to the function `sda` from the library `sparseLDA`; `sda` required 267 seconds to run and achieved an accuracy of 0.949. The maximum accuracy is achieved with the full regularization matrix, which is 0.957.

3.6 Commentary

Our proximal methods for sparse discriminant analysis provide a decrease in classification error over the existing LARS approach in almost all experiments, while we see a significant decrease in terms of computational resources used by the accelerated proximal gradient method (APG and APGB) and ADMM over LARS. This improvement in run time is most significant when applied to the Penicillium and synthetic data sets. Again, this is not a coincidence. The per-iteration complexity of these methods is on the order of $\mathcal{O}(p)$ floating point operations per-iteration, which leads to overall computation time, as measured in floating point operations, to be far less than the $\mathcal{O}(p^3)$ flops of the classical LARS method. The decrease in run time is most significant when p is large, as it is for the Penicillium data set, where the cost of $\mathcal{O}(p^3)$ flops for LARS is prohibitive. It is important to note that the slow convergence of the proximal gradient method (PG/PGB) without acceleration yields significantly longer run times despite the decreased per-iteration cost. We should also note that our use of cross validation can cause significant variation in the performance of our heuristics. This is because the trained discriminant vectors are sensitive to the split in the validation process. Finally, we note that there appears to be limited benefit from the use of backtracking line search, when compared to a constant step size given by the Frobenius norm estimate $\|\mathbf{A}\|_F$ of the Lipschitz constant. Specifically, the results of these experiments indicate that using a constant step length yields similar classification performance to the backtracking approach, but without a significant increase in run time due to repeated calculation of ∇f .

4 Conclusion

We have proposed new algorithms for solving the sparse optimal scoring problem for high-dimensional linear discriminant analysis based on block coordinate descent and proximal operator evaluations. We observe that

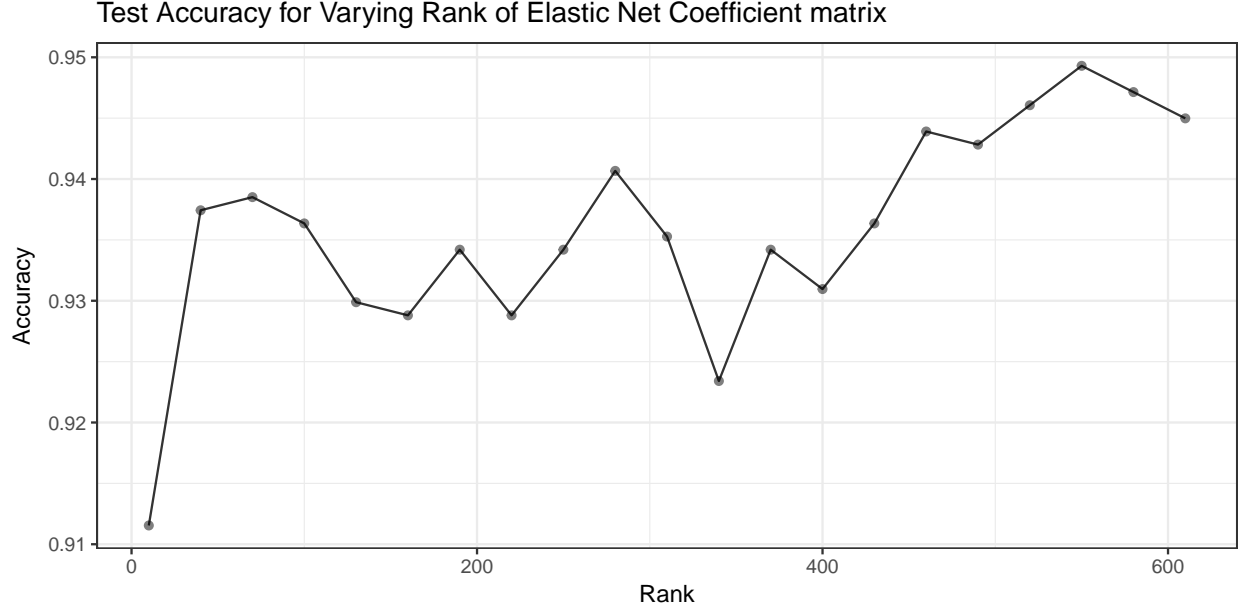


Figure 10: Test accuracy as function of $\text{rank}(\Omega)$

these algorithms provide significant improvement over existing approaches for solving the SOS problem in terms of efficiency and scalability. These improvements are most acute in the case that specially structured Tikhonov regularization is employed in the SOS formulation; for example, the computational resources required for each iteration scales linearly with the dimension of the data if either a diagonal or low-rank matrix is used. Moreover, we establish that any convergent subsequence of iterates generated by one of our algorithms converges to a stationary point. Finally, numerical simulation establishes that our approach provides an improvement over existing methods for sparse discriminant analysis in terms of both quality of solution and run time.

These results present several exciting avenues for future research. Although we focus primarily on the solution of the optimal scoring problem under regularization in the form of a generalized elastic net penalty, our approach should translate immediately to formulations with any nonsmooth convex penalty function. That is, the framework provided by Algorithm 1 can be applied to solve the SOS problem (2) obtained by applying an arbitrary convex penalty to the objective of the optimal scoring problem (1). The resulting optimization problem can be approximately solved by alternately minimizing with respect to the score vector θ using the formula (4) and with respect to the discriminant vector β by solving a modified version of (5). The proximal methods outlined in this paper can be applied to minimize with respect to β if the regularization function is convex, however it is unlikely that the computational resources necessary for this minimization will scale as favorably as with the generalized elastic net penalty. On the other hand, the convergence analysis presented in Section 2.5 extends immediately to this more general framework. Of particular interest is the modification of this approach to provide means of learning discriminant vectors for data containing ordinal labels, data containing corrupted or missing observations, and semi-supervised settings.

Finally, the results found in Section 2.5, as well as Appendices B and C establish that any convergent subsequence of iterates generated by our block coordinate descent approach must converge to a stationary point. However, it is still unclear when this sequence of iterates is convergent, or at what rate these subsequences converge; further study is required to better understand the convergence properties of these algorithms. Similarly, despite the empirical evidence provided in Section 3, it is unknown what conditions ensure that data is classifiable using sparse optimal scoring and, more generally, linear discriminant analysis. Extensive consistency analysis is needed to determine theoretical error rates for distinguishing random variables drawn from distinct distributions.

4.1 Acknowledgements

We are grateful to Mingyi Hong for his helpful comments and suggestions. B. Ames was supported in part by University of Alabama Research Grants RG14678 and RG14838. G. Einarsson’s PhD scholarship is funded by the Lundbeck foundation and the Technical University of Denmark. S. Atkins was part of the University Scholars Program at the University of Alabama while this research was conducted, and currently has a graduate student fellowship funded by the University of Florida.

References

- [1] Allen-Zhu, Z., Orecchia, L.: Linear coupling: An ultimate unification of gradient and mirror descent (2014)
- [2] Ames, B., Hong, M.: Alternating direction method of multipliers for penalized zero-variance discriminant analysis. *Computational Optimization and Applications* **64**(3), 725–754 (2016). DOI 10.1007/s10589-016-9828-y
- [3] Beck, A.: First-order methods in optimization, vol. 25. SIAM (2017)
- [4] Beck, A., Teboulle, M.: A fast iterative shrinkage-thresholding algorithm for linear inverse problems. *SIAM journal on imaging sciences* **2**(1), 183–202 (2009). DOI 10.1137/080716542
- [5] Boyd, S., Parikh, N., Chu, E., Peleato, B., Eckstein, J.: Distributed optimization and statistical learning via the alternating direction method of multipliers. *Foundations and Trends® in Machine Learning* **3**(1), 1–122 (2011). DOI 10.1561/22000000016
- [6] Bubeck, S., Lee, Y.T., Singh, M.: A geometric alternative to Nesterov’s accelerated gradient descent (2015)
- [7] Cai, T., Liu, W.: A direct estimation approach to sparse linear discriminant analysis. *Journal of the American Statistical Association* **106**(496), 1566–1577 (2011). DOI 10.1198/jasa.2011.tm11199
- [8] Chen, Y., Keogh, E., Hu, B., Begum, N., Bagnall, A., Mueen, A., Batista, G.: The ucr time series classification archive (2015). URL http://www.cs.ucr.edu/~eamonn/time_series_data/
- [9] Clemmensen, L., Hansen, M., Frisvad, J., Ersbøll, B.: A method for comparison of growth media in objective identification of penicillium based on multi-spectral imaging. *Journal of Microbiological Methods* **69**(2), 249–255 (2007). DOI 10.1016/j.mimet.2006.12.020
- [10] Clemmensen, L., Hastie, T., Witten, D., Ersbøll, B.: Sparse discriminant analysis. *Technometrics* **53**(4), 406–413 (2011). DOI 10.1198/TECH.2011.08118
- [11] Deng, W., Yin, W.: On the global and linear convergence of the generalized alternating direction method of multipliers. *Journal of Scientific Computing* **3**(66), 889–916 (2012). DOI 10.1007/s10915-015-0048-x
- [12] Einarsson, G., Clemmensen, L., Ames, B., Atkins, S.: accsda: Accelerated sparse discriminant analysis (2017). URL <https://cran.r-project.org/web/packages/accSDA/index.html>. Also available at <https://github.com/gumeo/accSDA>
- [13] Einarsson, G., Jensen, J.N., Paulsen, R.R., Einarisdottir, H., Ersbøll, B.K., Dahl, A.B., Christensen, L.B.: Foreign object detection in multispectral x-ray images of food items using sparse discriminant analysis. In: *Scandinavian Conference on Image Analysis*, pp. 350–361. Springer (2017)
- [14] Fan, J., Fan, Y.: High dimensional classification using features annealed independence rules. *Annals of Statistics* **36**(6), 2605–2637 (2008). DOI 10.1214/07-AOS504
- [15] Flammarion, N., Bach, F.: From averaging to acceleration, there is only a step-size (2015)
- [16] Friedman, J., Hastie, T., Tibshirani, R.: Regularization paths for generalized linear models via coordinate descent. *Journal of statistical software* **33**(1), 1 (2010)

- [17] Golub, G.H., Van Loan, C.F.: Matrix Computations, 4th edn. The Johns Hopkins University Press, Baltimore (2013)
- [18] Hastie, T., Tibshirani, R., Buja, A.: Flexible discriminant analysis by optimal scoring. *Journal of the American Statistical Association* **89**(428), 1255–1270 (1994). DOI 10.2307/2290989
- [19] Hastie, T., Tibshirani, R., Friedman, J.H.: The Elements of Statistical Learning, 2nd edn. Springer-Verlag New York, New York (2013)
- [20] Hastie, T., Tibshirani, R., Wainwright, M.: Statistical Learning with Sparsity: the Lasso and Generalizations, 1st edn. CRC Press, Boca Raton and London and New York (2012)
- [21] Lessard, L., Recht, B., Packard, A.: Analysis and design of optimization algorithms via integral quadratic constraints. *SIAM Journal on Optimization* **26**(1), 57–95 (2016). DOI 10.1137/15M1009597
- [22] Ma, Q., Yuan, M., Zou, H.: A direct approach to sparse discriminant analysis in ultra-high dimensions. *Biometrika* **99**, 29–42 (2012). DOI 10.1093/biomet/asr066
- [23] Mai, Q., Zou, H.: A note on the connection and equivalence of three sparse linear discriminant analysis methods. *Technometrics* **55**(2), 243–246 (2013). DOI 10.1080/00401706.2012.746208
- [24] Mai, Q., Zou, H.: Multiclass sparse discriminant analysis (2015)
- [25] Matérn, B.: Spatial variation, vol. 36. Springer Science & Business Media (2013)
- [26] Nesterov, Y.: A method of solving a convex programming problem with convergence rate $o(1/k^2)$. In: *Soviet Mathematics Doklady*, vol. 27, pp. 372–376 (1983). URL <http://mpawankumar.info/teaching/cdt-big-data/nesterov83.pdf>
- [27] Nesterov, Y.: Smooth minimization of non-smooth functions. *Mathematical programming* **103**(1), 127–152 (2005). DOI 10.1007/s10107-004-0552-5
- [28] Nesterov, Y.: Gradient methods for minimizing composite functions. *Mathematical Programming* **140**(1), 125–161 (2013). DOI 10.1007/s10107-012-0629-5
- [29] Nocedal, J., Wright, S.: Numerical optimization, 2nd edn. Springer Science & Business Media, New York (2006)
- [30] O’Donoghue, B., Candes, E.: Adaptive restart for accelerated gradient schemes. *Foundations of Computational Mathematics* **15**(3), 715–732 (2015). DOI 10.1007/s10208-013-9150-3
- [31] Parikh, N., Boyd, S.P.: Proximal algorithms. *Foundations and Trends in optimization* **1**(3), 127–239 (2014). DOI 10.1561/24000000003
- [32] Shao, J., Wang, Y., Deng, X., Wang, S.: Sparse linear discriminant analysis by thresholding for high dimensional data. *The Annals of Statistics* **39**(2), 1241–1265 (2011). DOI 10.1214/10-AOS870
- [33] Su, W., Boyd, S., Candes, E.: A differential equation for modeling nesterovs accelerated gradient method: Theory and insights. In: *Advances in Neural Information Processing Systems*, pp. 2510–2518 (2014)
- [34] Tibshirani, R., Hastie, T., Narasimhan, B., Chu, G.: Class prediction by nearest shrunken centroids, with applications to dna microarrays. *Statistical Science* pp. 104–117 (2003). DOI 10.1214/ss/1056397488
- [35] Tseng, P.: On accelerated proximal gradient methods for convex-concave optimization (2008). URL <http://www.mit.edu/~dimitrib/PTseng/papers/apgm.pdf>
- [36] Witten, D.M., Tibshirani, R.: Penalized classification using Fisher’s linear discriminant. *Journal of the Royal Statistical Society: Series B (Statistical Methodology)* **73**(5), 753–772 (2011). DOI 10.1111/j.1467-9868.2011.00783.x

- [37] Wu, M., Zhang, L., Wang, Z., Christiani, D., Lin, X.: Sparse linear discriminant analysis for simultaneous testing for the significance of a gene set/pathway and gene selection. *Bioinformatics* **25**(9), 1145–1151 (2008). DOI 10.1093/bioinformatics/btp019
- [38] Zou, H., Hastie, T.: Regularization and variable selection via the elastic net. *Journal of the Royal Statistical Society: Series B (Statistical Methodology)* **67**(2), 301–320 (2005). DOI 10.1111/j.1467-9868.2005.00503.x

A Proof of Lemma 2.1

We begin with a proof of Lemma 2.1, which provides a formula for the optimal solution of the θ -update subproblem (3).

Proof: We note that (3) has trivial solution $\theta = e$ for every $\beta = \beta^t \in \mathbf{R}^p$. Indeed, $Y e = e$ by the structure of the indicator matrix Y and $\sum_{i=1}^n x_{ij} = 0$ for all $j = 1, 2, \dots, p$ because our data has been centered to have sample mean equal to $\mathbf{0}$. This implies that (3) has the hidden constraint $\theta^T Y^T Y e = 0$. Therefore, we may reformulate (3) as

$$\begin{aligned} \min_{\theta \in \mathbf{R}^K} \quad & \|Y\theta - X\beta\|^2 \\ \text{s.t.} \quad & \theta^T Y^T Y \theta = n, \\ & \theta^T Y^T Y e = 0, \\ & \theta^T Y^T Y \theta_\ell = 0 \quad \ell < k. \end{aligned} \tag{27}$$

We wish to show that (27) has optimal solution $\hat{\theta}$ given by

$$\hat{\theta} = \frac{w}{\sqrt{w^T D w}}, \tag{28}$$

where $w = (I - Q_k Q_k^T D) D^{-1} Y^T X \beta$.

To do so, note that (27) satisfies the linear independence constraint qualification because the constraint gradients $\{2Y^T Y \theta, Y^T Y e, Y^T Y \theta_1, \dots, Y^T Y \theta_{k-1}\}$ are linearly independent. Moreover, the optimal value of (27) is bounded below by 0. Therefore, (27) has global minimizer, $\hat{\theta}$, which must satisfy the Karush-Kuhn-Tucker conditions, i.e., there exists $v \in \mathbf{R}^k$, $\psi \in \mathbf{R}$ such that

$$Y^T Y \hat{\theta} - Y^T X \beta + \psi Y^T Y \hat{\theta} + Y^T Y Q_k v = \mathbf{0}, \tag{29}$$

where $Q_k = [e, \theta_1, \theta_2, \dots, \theta_{k-1}]$. We consider the following two cases.

First, suppose that $Y^T X \beta \notin \text{range}(Y^T Y Q_k)$. Rearranging (29) yields

$$\hat{\theta} = \frac{1}{1 + \psi} (Y^T Y)^{-1} (Y^T X \beta - Y^T Y Q_k v). \tag{30}$$

We choose the dual variables ψ and v so that $\hat{\theta}$ is feasible for (27). It is easy to see that the conjugacy constraints are equivalent to $Q_k^T Y^T Y \hat{\theta} = \mathbf{0}$, which holds if and only if

$$\mathbf{0} = Q_k^T (Y^T X \beta - Y^T Y Q_k v) = Q_k^T Y^T X \beta - Q_k^T Y^T Y Q_k v = Q_k^T Y^T X \beta - n v,$$

where the last equality follows from the fact that $e^T Y^T Y e = \theta_i^T Y^T Y \theta_i = n$ for all $i = 1, 2, \dots, k-1$. It follows immediately that

$$v = \frac{1}{n} Q_k^T Y^T X \beta. \tag{31}$$

Substituting (31) into (30) yields

$$\begin{aligned}
\hat{\theta} &= \frac{1}{1+\psi} \left((\mathbf{Y}^T \mathbf{Y})^{-1} \mathbf{Y}^T \mathbf{X} \beta - \frac{1}{n} \mathbf{Q}_k \mathbf{Q}_k^T \mathbf{Y}^T \mathbf{X} \beta \right) \\
&= \frac{1}{n(1+\psi)} \left(\mathbf{D}^{-1} \mathbf{Y}^T \mathbf{X} \beta - \mathbf{Q}_k \mathbf{Q}_k^T \mathbf{Y}^T \mathbf{X} \beta \right) \\
&= \frac{1}{n(1+\psi)} \left(\mathbf{I} - \mathbf{Q}_k \mathbf{Q}_k^T \mathbf{D} \right) \mathbf{D}^{-1} \mathbf{Y}^T \mathbf{X} \beta \\
&= \frac{1}{n(1+\psi)} \mathbf{w},
\end{aligned} \tag{32}$$

where $\mathbf{D} = \frac{1}{n} \mathbf{Y}^T \mathbf{Y}$ and we choose $\psi \in \mathbf{R}$ so that $\hat{\theta}^T \mathbf{D} \hat{\theta} = 1$:

$$n(1+\psi) = \pm \sqrt{\mathbf{w}^T \mathbf{D} \mathbf{w}}. \tag{33}$$

To complete the argument, note that

$$\|\mathbf{Y} \hat{\theta} - \mathbf{X} \beta\|^2 = n \mp \frac{2}{\sqrt{\mathbf{w}^T \mathbf{D} \mathbf{w}}} \beta^T \mathbf{X}^T \mathbf{Y} (\mathbf{D}^{-1} - \mathbf{Q}_k \mathbf{Q}_k^T) \mathbf{Y}^T \mathbf{X} \beta + \beta^T \mathbf{X}^T \mathbf{X} \beta.$$

Note further that the matrix $\mathbf{Y} \mathbf{Q}_k \mathbf{Q}_k^T \mathbf{Y}^T$ has decomposition

$$\mathbf{Y} \mathbf{Q}_k \mathbf{Q}_k^T \mathbf{Y}^T = \mathbf{Y} \mathbf{e} \mathbf{e}^T \mathbf{Y}^T + \mathbf{Y} \boldsymbol{\theta}_1 \boldsymbol{\theta}_1^T \mathbf{Y}^T + \cdots + \mathbf{Y} \boldsymbol{\theta}_{k-1} \boldsymbol{\theta}_{k-1}^T \mathbf{Y}^T.$$

The conjugacy of the columns of \mathbf{Q}_k implies that eigenvectors of $\mathbf{Y} \mathbf{Q}_k \mathbf{Q}_k^T \mathbf{Y}^T$ are $\mathbf{Y} \boldsymbol{\theta}_1, \dots, \mathbf{Y} \boldsymbol{\theta}_{k-1}$, and $\mathbf{Y} \mathbf{e}$, each with eigenvalue n ; since $\text{rank}(\mathbf{Y} \mathbf{Q}_k \mathbf{Q}_k^T \mathbf{Y}^T) = k$, all remaining eigenvalues of $\mathbf{Y} \mathbf{Q}_k \mathbf{Q}_k^T \mathbf{Y}^T$ must be equal to 0. Moreover, for any $\mathbf{z} = \mathbf{Y} \boldsymbol{\theta}_i$, $i = 1, 2, \dots, k-1$, or $\mathbf{z} = \mathbf{Y} \mathbf{e}$, we have

$$\mathbf{Y} (\mathbf{D}^{-1} - \mathbf{Q}_k \mathbf{Q}_k^T) \mathbf{Y}^T \mathbf{z} = (n - n) \mathbf{z} = 0.$$

The matrix \mathbf{D}^{-1} is a positive definite diagonal matrix, with i th diagonal entry $n/|C_i|$, where $|C_i|$ denotes the number of observations belonging to class i ; this implies that $\mathbf{Y} \mathbf{D}^{-1} \mathbf{Y}^T$ is positive semidefinite. This establishes that the matrix $\mathbf{Y} (\mathbf{D}^{-1} - \mathbf{Q}_k \mathbf{Q}_k^T) \mathbf{Y}^T$ is positive semidefinite and thus $\|\mathbf{Y} \hat{\theta} - \mathbf{X} \beta\|^2$ is minimized by $\hat{\theta}$ with $\psi = +\sqrt{\mathbf{w}^T \mathbf{D} \mathbf{w}}/n - 1$.

Second, suppose that $\mathbf{Y}^T \mathbf{X} \beta \in \text{range}(\mathbf{Y}^T \mathbf{Y} \mathbf{Q}_k)$. This implies that there exists some $\mathbf{v} \in \mathbf{R}^k$ such that

$$\mathbf{Y}^T \mathbf{X} \beta = \mathbf{Y}^T \mathbf{Y} \mathbf{Q}_k \mathbf{v}.$$

Substituting into the objective of (27), we see that

$$\begin{aligned}
\|\mathbf{Y} \boldsymbol{\theta} - \mathbf{X} \beta\|^2 &= \boldsymbol{\theta}^T \mathbf{Y}^T \mathbf{Y} \boldsymbol{\theta} - 2 \boldsymbol{\theta}^T \mathbf{Y}^T \mathbf{X} \beta + \beta^T \mathbf{X}^T \mathbf{X} \beta \\
&= n - 2 \boldsymbol{\theta}^T \mathbf{Y}^T \mathbf{Y} \mathbf{Q}_k \mathbf{v} + \beta^T \mathbf{X}^T \mathbf{X} \beta \\
&= n + \beta^T \mathbf{X}^T \mathbf{X} \beta
\end{aligned}$$

for every feasible solution $\boldsymbol{\theta}$ of (27). This implies that every feasible solution of (27) is also optimal in this case. In particular, $\hat{\theta}$ given by (32) is feasible for (27) and, therefore, optimal. \blacksquare

B Proof of Theorem 2.4

We next prove Theorem 2.4, which establishes that Algorithm 1 converges in function value.

Proof: Suppose that, after t iterations, we have iterates $(\boldsymbol{\theta}^t, \boldsymbol{\beta}^t)$ with objective function value $F(\boldsymbol{\theta}^t, \boldsymbol{\beta}^t)$. Recall that we obtain $\boldsymbol{\beta}^{t+1}$ as the solution of (5). Moreover, note that $\boldsymbol{\beta}^t$ is also feasible for (5). This immediately implies that

$$F(\boldsymbol{\theta}^t, \boldsymbol{\beta}^t) \geq F(\boldsymbol{\theta}^t, \boldsymbol{\beta}^{t+1}).$$

On the other hand, $\boldsymbol{\theta}^{t+1}$ is the solution of (3) with $\boldsymbol{\beta} = \boldsymbol{\beta}^{t+1}$. Therefore, we have

$$F(\boldsymbol{\theta}^t, \boldsymbol{\beta}^t) \geq F(\boldsymbol{\theta}^t, \boldsymbol{\beta}^{t+1}) \geq F(\boldsymbol{\theta}^{t+1}, \boldsymbol{\beta}^{t+1}).$$

It follows that the sequence of function values $\{F(\boldsymbol{\theta}^t, \boldsymbol{\beta}^t)\}_{t=1}^\infty$ is nonincreasing. Moreover, the objective function $F(\boldsymbol{\theta}, \boldsymbol{\beta})$ is nonnegative for all $\boldsymbol{\theta}$ and $\boldsymbol{\beta}$. Therefore, $\{F(\boldsymbol{\theta}^t, \boldsymbol{\beta}^t)\}_{t=1}^\infty$ is convergent as a monotonic bounded sequence. ■

C Proof of Theorem 2.5

To prove Theorem 2.5, we first establish the following lemma, which establishes that the limit point $(\boldsymbol{\theta}^*, \boldsymbol{\beta}^*)$ minimizes F with respect to each primal variable with the other fixed; that is, $\boldsymbol{\theta}^*$ minimizes $F(\cdot, \boldsymbol{\beta}^*)$ and $\boldsymbol{\beta}^*$ minimizes $F(\boldsymbol{\theta}^*, \cdot)$.

Lemma C.1 *Let $\{(\boldsymbol{\theta}^t, \boldsymbol{\beta}^t)\}_{t=1}^\infty$ be the sequence of points generated by Algorithm 1. Suppose that $\{(\boldsymbol{\theta}^{t_j}, \boldsymbol{\beta}^{t_j})\}_{j=1}^\infty$ is a convergent subsequence of $\{(\boldsymbol{\theta}^t, \boldsymbol{\beta}^t)\}_{t=1}^\infty$ with limit $(\boldsymbol{\theta}^*, \boldsymbol{\beta}^*)$. Then*

$$F(\boldsymbol{\theta}, \boldsymbol{\beta}^*) \geq F(\boldsymbol{\theta}^*, \boldsymbol{\beta}^*) \quad (34)$$

$$F(\boldsymbol{\theta}^*, \boldsymbol{\beta}) \geq F(\boldsymbol{\theta}^*, \boldsymbol{\beta}^*) \quad (35)$$

for all feasible $\boldsymbol{\theta} \in \mathbf{R}^k$ and $\boldsymbol{\beta} \in \mathbf{R}^p$.

Proof: We first establish (35). Consider $(\boldsymbol{\theta}^{t_j}, \boldsymbol{\beta}^{t_j})$. By our update step for $\boldsymbol{\beta}$, we note that

$$\boldsymbol{\beta}^{t_j} = \arg \min_{\boldsymbol{\beta} \in \mathbf{R}^p} F(\boldsymbol{\theta}^{t_j}, \boldsymbol{\beta}).$$

Thus, for all $j = 1, 2, \dots$, we have $F(\boldsymbol{\theta}^{t_j}, \boldsymbol{\beta}) \geq F(\boldsymbol{\theta}^{t_j}, \boldsymbol{\beta}^{t_j})$ for all $\boldsymbol{\beta} \in \mathbf{R}^p$. Taking the limit as $j \rightarrow \infty$ and using the continuity of F establishes (35).

Next, note that, for every $j = 1, 2, \dots$, we have

$$\begin{aligned} \boldsymbol{\theta}^{t_j+1} &= \arg \min_{\boldsymbol{\theta} \in \mathbf{R}^k} F(\boldsymbol{\theta}, \boldsymbol{\beta}^{t_j}) \\ \text{s.t. } &\boldsymbol{\theta}^T \mathbf{Y}^T \mathbf{Y} \boldsymbol{\theta} = n, \quad \boldsymbol{\theta}^T \mathbf{Y}^T \mathbf{Y} \boldsymbol{\theta}_\ell = 0 \quad \forall \ell < k. \end{aligned}$$

This implies that

$$F(\boldsymbol{\theta}, \boldsymbol{\beta}^{t_j}) \geq F(\boldsymbol{\theta}^{t_j+1}, \boldsymbol{\beta}^{t_j}) \geq F(\boldsymbol{\theta}^{t_j+1}, \boldsymbol{\beta}^{t_j+1}) \geq F(\boldsymbol{\theta}^{t_{j+1}}, \boldsymbol{\beta}^{t_{j+1}})$$

by the monotonicity of the sequence of function values and the fact that $t_j < t_j + 1 \leq t_{j+1}$. Taking the limit as $j \rightarrow \infty$ and using the continuity of F establishes (34). This completes the proof of Lemma C.1. ■

We are now ready to prove Theorem 2.5. **Proof:** of Theorem 2.5 The form of the subdifferential of L implies that $(\mathbf{g}_\theta, \mathbf{g}_\beta) \in \partial L(\boldsymbol{\theta}, \boldsymbol{\beta}, \psi, \mathbf{v})$ if and only if

$$\mathbf{g}_\theta = 2(1 + \psi) \mathbf{Y}^T \mathbf{Y} \boldsymbol{\theta} - 2 \mathbf{Y}^T \mathbf{X} \boldsymbol{\beta} + \mathbf{U}^T \mathbf{v} \quad (36)$$

$$\mathbf{g}_\beta \in 2(\mathbf{X}^T \mathbf{X} + \gamma \boldsymbol{\Omega}) \boldsymbol{\beta} - 2 \mathbf{X}^T \mathbf{Y} \boldsymbol{\theta} + \lambda \partial \|\boldsymbol{\beta}\|_1 \quad (37)$$

for all $\mathbf{v} \in \mathbf{R}^{k-1}$ and $\psi \in \mathbf{R}$. It is easy to see from (35) that $\boldsymbol{\beta}^* = \arg \min_{\boldsymbol{\beta} \in \mathbf{R}^p} F(\boldsymbol{\theta}^*, \boldsymbol{\beta})$. Thus, by the first order necessary conditions for unconstrained convex optimization, we must have

$$\begin{aligned} \mathbf{0} &\in \partial \left(\frac{1}{2} (\boldsymbol{\beta}^*)^T \mathbf{A} \boldsymbol{\beta}^* + \mathbf{d}^T \boldsymbol{\beta}^* + \lambda \|\boldsymbol{\beta}^*\|_1 \right) \\ &= 2(\mathbf{X}^T \mathbf{X} + \gamma \boldsymbol{\Omega}) \boldsymbol{\beta}^* - 2 \mathbf{X}^T \mathbf{Y} \boldsymbol{\theta}^* + \lambda \partial \|\boldsymbol{\beta}^*\|_1; \end{aligned} \quad (38)$$

here $\partial \|\boldsymbol{\beta}\|_1$ denotes the subdifferential of the ℓ_1 -norm at the point $\boldsymbol{\beta}$.

On the other hand, (34) implies

$$\begin{aligned} \boldsymbol{\theta}^* = \arg \min_{\boldsymbol{\theta} \in \mathbf{R}^K} \quad & \|\mathbf{Y}\boldsymbol{\theta} - \mathbf{X}\boldsymbol{\beta}^*\|^2 \\ \text{s.t.} \quad & \boldsymbol{\theta}^T \mathbf{Y}^T \mathbf{Y} \boldsymbol{\theta} = n, \quad 2\boldsymbol{\theta}^T \mathbf{Y}^T \mathbf{Y} \boldsymbol{\theta}_\ell = 0, \quad \forall \ell < k. \end{aligned} \quad (39)$$

Moreover, the problem (39) satisfies the linear independence constraint qualification. Indeed, the set of active constraint gradients $\{2\mathbf{Y}^T \mathbf{Y} \boldsymbol{\theta}, 2\mathbf{Y}^T \mathbf{Y} \boldsymbol{\theta}_1, \dots, 2\mathbf{Y}^T \mathbf{Y} \boldsymbol{\theta}_{k-1}\}$ is linearly independent for any feasible $\boldsymbol{\theta} \in \mathbf{R}^K$ by the $\mathbf{Y}^T \mathbf{Y}$ -conjugacy of $\{\boldsymbol{\theta}, \boldsymbol{\theta}_1, \dots, \boldsymbol{\theta}_{k-1}\}$. Therefore, there exist Lagrange multipliers ψ^*, \mathbf{v}^* such that

$$\mathbf{0} = 2(1 + \psi^*)\mathbf{Y}^T \mathbf{Y} \boldsymbol{\theta}^* - 2\mathbf{Y}^T \mathbf{X} \boldsymbol{\beta}^* + \mathbf{U}^T \mathbf{v}^* \quad (40)$$

by the first-order necessary conditions for optimality (see [29, Theorem 12.1]). We see that $\mathbf{0} \in \partial L(\boldsymbol{\theta}^*, \boldsymbol{\beta}^*, \psi^*, \mathbf{v}^*)$ by combining (38) and (40). This completes the proof. \blacksquare

D Additional Numerical Results

We conclude by providing full numerical results from the experiments described in Section 3.1 and Section 3.2. These are located in Table 5, Table 6, and Table 7.

Table 5: Comparison of classification performance of benchmarking data. Each block reports the number of classification errors on out-of-sample testing observations (numErr), fraction of classification errors (fracErr), number of nonzero features used for classification (feats), fraction of nonzero features (fracFeat), and time (in seconds) needed to train the discriminant vectors (runTime).

Dataset	Measures	PG	PGB	APG	APGB	ADMM	SZVD	LARS
Pen p=3542 K=3 ntrain=24 ntest=12	numErr	0.00e+00	0.00e+00	0.00e+00	0.00e+00	0.00e+00	0.00e+00	1.00e+00
	fracErr	0.00e+00	0.00e+00	0.00e+00	0.00e+00	0.00e+00	0.00e+00	8.33e-02
	numFeat	3.35e+02	3.36e+02	2.82e+02	2.42e+02	8.84e+02	2.33e+03	3.58e+02
	fracFeat	4.73e-02	4.74e-02	3.98e-02	3.42e-02	1.25e-01	3.28e-01	5.05e-02
	runTime	4.16e+02	2.33e+04	4.05e+01	1.54e+02	5.94e+02	3.46e+04	4.35e+04
ECG p=136 K=2 ntrain=23 ntest=861	numErr	8.70e+01	3.50e+01	1.01e+02	8.10e+01	1.80e+01	2.40e+01	1.30e+02
	fracErr	1.01e-01	4.07e-02	1.17e-01	9.41e-02	2.09e-02	2.79e-02	1.51e-01
	numFeat	1.50e+01	2.10e+01	1.00e+01	1.20e+01	2.50e+01	1.15e+02	4.00e+00
	fracFeat	1.10e-01	1.54e-01	7.35e-02	8.82e-02	1.84e-01	8.46e-01	2.94e-02
	runTime	1.03e+01	1.04e+01	4.05e+00	1.73e+01	2.40e+01	2.32e+00	2.70e+00
Coffee p=286 K=2 ntrain=28 ntest=28	numErr	0.00e+00	0.00e+00	0.00e+00	0.00e+00	0.00e+00	0.00e+00	0.00e+00
	fracErr	0.00e+00	0.00e+00	0.00e+00	0.00e+00	0.00e+00	0.00e+00	0.00e+00
	numFeat	3.30e+01	3.30e+01	3.50e+01	3.60e+01	6.80e+01	2.08e+02	8.00e+00
	fracFeat	1.15e-01	1.15e-01	1.22e-01	1.26e-01	2.38e-01	7.27e-01	2.80e-02
	runTime	7.12e+01	1.46e+03	8.52e+00	3.71e+01	4.95e+01	1.38e+01	7.48e+00
Olive Oil p=570 K=4 ntrain=30 ntest=30	numErr	2.00e+00	2.00e+00	4.00e+00	3.00e+00	1.00e+00	1.00e+00	1.00e+00
	fracErr	6.67e-02	6.67e-02	1.33e-01	1.00e-01	3.33e-02	3.33e-02	3.33e-02
	numFeat	1.15e+02	9.50e+01	6.90e+01	7.30e+01	2.25e+02	9.93e+02	1.33e+02
	fracFeat	1.93e-01	1.61e-01	1.19e-01	1.26e-01	3.18e-01	9.32e-01	1.93e-01
	runTime	4.48e+02	3.26e+04	8.20e+01	3.44e+02	5.29e+02	7.67e+02	1.02e+03

Table 6: Results for synthetic data with $K = 2$. All results are listed in the format “mean (standard deviation)”. Bold entries indicate minimum average values for each statistic and data set. In all experiments, $n_{train} = 25K$ and $n_{test} = 250K$.

Dataset	Measures	PG	PGB	APG	APGB	ADMM	SZVD	LARS
p=500 r=0 K=2	numErr	6.00e-01 (1.07e+00)	2.80e+00 (5.65e+00)	6.00e-01 (5.16e-01)	3.50e+00 (1.65e+00)	0.00e+00 (0.00e+00)	1.00e-01 (3.16e-01)	9.13e+01 (1.66e+01)
	fracErr	1.20e-03 (2.15e-03)	5.60e-03 (1.13e-02)	1.20e-03 (1.03e-03)	7.00e-03 (3.30e-03)	0.00e+00 (0.00e+00)	2.00e-04 (6.32e-04)	1.83e-01 (3.33e-02)
	numFeat	1.33e+02 (3.37e+01)	1.22e+02 (4.45e+01)	1.35e+02 (1.06e+01)	1.23e+02 (1.08e+01)	2.19e+02 (1.93e+01)	1.69e+02 (1.41e+01)	1.30e+01 (0.00e+00)
	fracFeat	2.65e-01 (6.74e-02)	2.45e-01 (8.90e-02)	2.71e-01 (2.13e-02)	2.46e-01 (2.17e-02)	4.38e-01 (3.86e-02)	3.38e-01 (2.81e-02)	2.60e-02 (0.00e+00)
	runTime	5.08e+00 (7.19e-01)	1.94e+03 (2.91e+02)	2.96e+00 (2.53e-01)	2.86e+01 (2.46e+00)	3.98e+01 (1.97e+00)	4.09e+01 (2.05e+00)	1.73e+01 (6.24e-01)
p=500 r=0.1 K=2	numErr	5.00e-01 (8.50e-01)	1.00e+00 (1.05e+00)	4.00e-01 (5.16e-01)	2.00e+00 (1.49e+00)	0.00e+00 (0.00e+00)	1.00e-01 (3.16e-01)	9.13e+01 (1.70e+01)
	fracErr	1.00e-03 (1.70e-03)	2.00e-03 (2.11e-03)	8.00e-04 (1.03e-03)	4.00e-03 (2.98e-03)	0.00e+00 (0.00e+00)	2.00e-04 (6.32e-04)	1.83e-01 (3.40e-02)
	numFeat	1.41e+02 (3.21e+01)	1.18e+02 (3.85e+01)	1.76e+02 (1.15e+02)	1.66e+02 (1.18e+02)	2.28e+02 (7.36e+00)	1.65e+02 (7.42e+00)	1.30e+01 (0.00e+00)
	fracFeat	2.82e-01 (6.41e-02)	2.36e-01 (7.69e-02)	3.51e-01 (2.29e-01)	3.31e-01 (2.35e-01)	4.56e-01 (1.47e-02)	3.30e-01 (1.48e-02)	2.60e-02 (0.00e+00)
	runTime	5.73e+00 (6.16e-01)	1.92e+03 (2.42e+02)	3.24e+00 (1.38e-01)	2.88e+01 (2.23e+00)	3.99e+01 (1.42e+00)	4.10e+01 (2.02e+00)	1.71e+01 (6.46e-01)
p=500 r=0.5 K=2	numErr	1.00e-01 (3.16e-01)	0.00e+00 (0.00e+00)	0.00e+00 (0.00e+00)	0.00e+00 (0.00e+00)	0.00e+00 (0.00e+00)	0.00e+00 (0.00e+00)	5.48e+01 (2.02e+01)
	fracErr	2.00e-04 (6.32e-04)	0.00e+00 (0.00e+00)	0.00e+00 (0.00e+00)	0.00e+00 (0.00e+00)	0.00e+00 (0.00e+00)	0.00e+00 (0.00e+00)	1.10e-01 (4.03e-02)
	numFeat	1.17e+02 (3.40e+01)	1.16e+02 (2.34e+01)	2.85e+02 (1.85e+02)	3.57e+02 (1.85e+02)	2.34e+02 (8.73e+00)	1.75e+02 (8.25e+00)	1.30e+01 (0.00e+00)
	fracFeat	2.34e-01 (6.80e-02)	2.32e-01 (4.67e-02)	5.71e-01 (3.71e-01)	7.13e-01 (3.70e-01)	4.69e-01 (1.75e-02)	3.50e-01 (1.65e-02)	2.60e-02 (0.00e+00)
	runTime	1.63e+01 (1.86e+00)	2.05e+03 (3.83e+02)	4.86e+00 (4.29e-01)	3.17e+01 (1.09e+00)	4.60e+01 (9.28e-01)	4.58e+01 (1.15e+00)	1.90e+01 (7.45e-01)
p=500 r=0.9 K=2	numErr	0.00e+00 (0.00e+00)	0.00e+00 (0.00e+00)	0.00e+00 (0.00e+00)	0.00e+00 (0.00e+00)	0.00e+00 (0.00e+00)	0.00e+00 (0.00e+00)	3.40e+00 (5.30e+00)
	fracErr	0.00e+00 (0.00e+00)	0.00e+00 (0.00e+00)	0.00e+00 (0.00e+00)	0.00e+00 (0.00e+00)	0.00e+00 (0.00e+00)	0.00e+00 (0.00e+00)	6.80e-03 (1.06e-02)
	numFeat	1.18e+02 (4.80e+01)	1.07e+02 (3.80e+01)	9.25e+01 (1.90e+01)	1.15e+02 (2.73e+01)	1.93e+02 (3.07e+00)	1.76e+02 (5.13e+00)	1.30e+01 (0.00e+00)
	fracFeat	2.36e-01 (9.59e-02)	2.14e-01 (7.59e-02)	1.85e-01 (3.80e-02)	2.29e-01 (5.46e-02)	3.86e-01 (6.14e-03)	3.52e-01 (1.03e-02)	2.60e-02 (0.00e+00)
	runTime	1.95e+01 (2.73e+00)	1.80e+03 (3.11e+02)	3.99e+00 (3.69e-01)	2.44e+01 (1.71e+00)	5.38e+01 (2.06e+00)	4.58e+01 (1.94e+00)	2.03e+01 (1.27e+00)

Table 7: Results for synthetic data with $K = 4$. All results are listed in the format “mean (standard deviation)”. Bold entries indicate minimum average values for each statistic and data set. In all experiments, $n_{train} = 25K$ and $n_{test} = 250K$.

Dataset	Measures	PG	PGB	APG	APGB	ADMM	SZVD	LARS
p=500 r=0 K=4	numErr	1.50e+01 (1.13e+01)	1.83e+01 (1.59e+01)	1.85e+01 (7.60e+00)	4.00e+01 (1.89e+01)	5.90e+00 (5.69e+00)	2.90e+00 (1.37e+00)	1.01e+02 (9.91e+00)
	fracErr	1.50e-02 (1.13e-02)	1.83e-02 (1.59e-02)	1.85e-02 (7.60e-03)	4.00e-02 (1.89e-02)	5.90e-03 (5.69e-03)	2.90e-03 (1.37e-03)	1.01e-01 (9.91e-03)
	numFeat	3.78e+02 (1.47e+02)	3.86e+02 (1.49e+02)	3.56e+02 (1.16e+02)	3.75e+02 (3.97e+01)	5.72e+02 (5.09e+01)	8.48e+02 (1.08e+02)	1.14e+02 (0.00e+00)
	fracFeat	5.85e-01 (1.42e-01)	5.89e-01 (1.58e-01)	5.64e-01 (1.19e-01)	5.92e-01 (3.58e-02)	7.68e-01 (3.61e-02)	9.23e-01 (3.38e-02)	2.22e-01 (4.16e-03)
p=500 r=0.1 K=4	runTime	1.33e+01 (9.68e-01)	7.26e+03 (4.89e+02)	1.47e+01 (6.24e-01)	1.86e+02 (5.66e+00)	2.28e+02 (9.09e+00)	2.05e+02 (8.80e+00)	3.61e+02 (2.25e+01)
	numErr	1.81e+01 (1.99e+01)	2.96e+01 (1.16e+01)	2.90e+01 (1.35e+01)	4.23e+01 (2.05e+01)	4.30e+00 (3.33e+00)	2.00e+00 (1.89e+00)	1.49e+02 (1.25e+01)
	fracErr	1.81e-02 (1.99e-02)	2.96e-02 (1.16e-02)	2.90e-02 (1.35e-02)	4.23e-02 (2.05e-02)	4.30e-03 (3.33e-03)	2.00e-03 (1.89e-03)	1.49e-01 (1.25e-02)
	numFeat	4.14e+02 (1.39e+02)	3.05e+02 (6.44e+01)	3.29e+02 (8.69e+01)	3.78e+02 (5.97e+01)	5.97e+02 (4.98e+01)	8.49e+02 (1.09e+02)	1.14e+02 (3.16e-01)
p=500 r=0.5 K=4	fracFeat	6.12e-01 (1.33e-01)	5.02e-01 (7.52e-02)	5.28e-01 (9.06e-02)	5.85e-01 (6.68e-02)	7.86e-01 (3.81e-02)	9.19e-01 (3.88e-02)	2.21e-01 (4.02e-03)
	runTime	1.50e+01 (1.09e+00)	6.68e+03 (3.20e+02)	1.61e+01 (6.12e-01)	1.83e+02 (6.60e+00)	2.32e+02 (5.39e+00)	2.07e+02 (5.57e+00)	3.69e+02 (1.41e+01)
	numErr	4.20e+00 (3.68e+00)	3.20e+00 (2.90e+00)	2.60e+00 (2.27e+00)	7.80e+00 (8.65e+00)	4.00e-01 (1.26e+00)	1.00e+00 (3.16e+00)	5.77e+01 (1.20e+01)
	fracErr	4.20e-03 (3.68e-03)	3.20e-03 (2.90e-03)	2.60e-03 (2.27e-03)	7.80e-03 (8.65e-03)	4.00e-04 (1.26e-03)	1.00e-03 (3.16e-03)	5.77e-02 (1.20e-02)
p=500 r=0.9 K=4	numFeat	3.04e+02 (3.64e+01)	3.07e+02 (2.14e+01)	3.16e+02 (2.04e+01)	4.04e+02 (1.00e+02)	4.86e+02 (6.46e+01)	9.44e+02 (2.14e+02)	1.14e+02 (3.16e-01)
	fracFeat	4.94e-01 (4.32e-02)	5.02e-01 (2.52e-02)	5.13e-01 (2.21e-02)	5.90e-01 (9.75e-02)	6.74e-01 (6.12e-02)	9.24e-01 (5.26e-02)	2.16e-01 (3.33e-03)
	runTime	4.57e+01 (5.82e+00)	6.88e+03 (7.06e+02)	2.23e+01 (1.72e+00)	1.83e+02 (6.03e+00)	2.43e+02 (1.00e+01)	2.06e+02 (8.72e+00)	3.63e+02 (2.25e+01)
	numErr	2.00e+00 (2.98e+00)	1.60e+00 (3.13e+00)	3.20e+00 (3.74e+00)	1.00e+00 (1.63e+00)	0.00e+00 (0.00e+00)	0.00e+00 (0.00e+00)	2.00e-01 (4.22e-01)
p=500 r=0.9 K=4	fracErr	2.00e-03 (2.98e-03)	1.60e-03 (3.13e-03)	3.20e-03 (3.74e-03)	1.00e-03 (1.63e-03)	0.00e+00 (0.00e+00)	0.00e+00 (0.00e+00)	2.00e-04 (4.22e-04)
	numFeat	2.40e+02 (1.54e+02)	2.20e+02 (1.13e+02)	1.90e+02 (3.91e+01)	2.27e+02 (7.00e+01)	5.28e+02 (5.16e+01)	1.02e+03 (1.66e+02)	1.14e+02 (3.16e-01)
	fracFeat	1.60e-01 (1.02e-01)	1.46e-01 (7.53e-02)	1.27e-01 (2.60e-02)	1.51e-01 (4.67e-02)	3.52e-01 (3.44e-02)	6.79e-01 (1.10e-01)	7.61e-02 (2.11e-04)
	runTime	5.74e+01 (6.05e+00)	6.00e+03 (4.22e+02)	2.05e+01 (1.16e+00)	1.60e+02 (5.83e+00)	2.74e+02 (3.92e+00)	2.09e+02 (4.42e+00)	3.86e+02 (1.76e+01)